Ecology Letters, (2008) **11**: 820–830 doi: 10.1111/j.1461-0248.2008.01194.x

LETTER

Colour of environmental noise affects the nonlinear dynamics of cycling, stage-structured populations

Daniel C. Reuman,[1]* Robert F. Costantino,[2] Robert A. Desharnais[3] and Joel E. Cohen[4]

[1]*Laboratory of Populations, The Rockefeller University, Box 20, 1230 York Avenue, New York, NY 10065, USA*

[2]*Department of Ecology and Evolutionary Biology, University of Arizona, Tucson, AZ 85721, USA*

[3]*Department of Biological Sciences, California State University, Los Angeles, CA 90032, USA*

[4]*Laboratory of Populations, Rockefeller and Columbia Universities, Box 20, 1230 York Avenue, New York, NY 10065, USA*

**Correspondence and present address: Imperial College London, Silwood Park Campus, Buckhurst Road, Ascot, Berkshire SL5 7PY, UK. E-mail: d.reuman@imperial.ac.uk*

Abstract

Populations fluctuate because of their internal dynamics, which can be nonlinear and stochastic, and in response to environmental variation. Theory predicts how the colour of environmental stochasticity affects population means, variances and correlations with the environment over time. The theory has not been tested for cycling populations, commonly observed in field systems. We applied noise of different colours to cycling laboratory beetle populations, holding other statistical properties of the noise fixed. Theory was largely validated, but failed to predict observations in sufficient detail. The main period of population cycling was shifted up to 33% by the colour of environmental stochasticity. Noise colour affected population means, variances and dominant periodicities differently for populations that cycled in different ways without noise. Our results show that changes in the colour of climatic variability, partly caused by humans, may affect the main periodicity of cycling populations, possibly impacting industry, pest management and conservation.

Keywords

Coloured noise, filter, flour beetle, nonlinear dynamics, population cycling, population dynamics, power spectrum, red noise, stage-structured, *Tribolium*.

Ecology Letters (2008) 11: 820–830

INTRODUCTION

The effects of the colour of environmental stochasticity on population and community dynamics are important but poorly understood. Population time series are often 'reddened', i.e. dominated by low-frequency oscillations (Ariño & Pimm 1995; Inchausti & Halley 2002). Some authors have argued that reddening is caused by fluctuations in stochastic environmental factors such as temperature and precipitation (Pimm & Redfearn 1988; Sugihara 1995), which are also often reddened (Vasseur & Yodzis 2004). Other causes of population reddening have been proposed (Kaitala & Ranta 1996; White *et al.* 1996; Greenman & Benton 2005a). Theory has predicted that the effects of noise colour on population means, variances, persistence times and power spectra can be substantial and complex (e.g. May 1973, 1981; Roughgarden 1975; Kaitala *et al.* 1997; Petchey *et al.* 1997; Morales 1999; Ripa & Ives 2003; Xu & Li 2003; Laakso *et al.* 2001, 2003a; Greenman & Benton 2003, 2005a,b; Schwager *et al.* 2006). However, most dynamical models assume that populations are affected by white noise. Fitting such models to data generated under the influence of reddened stochasticity leads to systematic errors (Ranta *et al.* 2000; Jonzén *et al.* 2002).

Models of the dynamics, in the presence of noise, of a species that would come to equilibrium in the absence of noise have been studied (e.g. Nisbet *et al.* 1977; Nisbet & Gurney 1982; Ripa *et al.* 1998; Petchey 2000; Ripa & Ives 2003; Laakso *et al.* 2003b; Bjørnstad *et al.* 2004; Greenman & Benton 2003, 2005a,b). Theoretical predictions for a single species that comes to equilibrium in the absence of noise include: (1) populations correlate better with red environmental fluctuations than with white or blue fluctuations; (2) populations with higher intrinsic growth rate, r, correlate better with the environment than do low-r populations; (3) the colour of environmental stochasticity tinges the colour of

population fluctuations; (4) populations affected by red noise are more variable than populations affected by noise of other colours and (5) high-*r* populations are more variable than low-*r* populations in the presence of noise but (6) less variable in constant environments (May 1973, 1981; Roughgarden 1975; Pimm & Redfearn 1988; Sugihara 1995; Kaitala *et al.* 1997). We use these predictions as a benchmark, testing how well they hold for a system that does not come to equilibrium in the absence of noise.

Two laboratory experiments on ciliates (Petchey 2000; Laakso *et al.* 2003b) tested the theory. Several studies, including Luckinbill & Fenton (1978) and Jillson (1980), tested the effects of deterministic environmental forcing of various periods. We know no prior controlled experiments on the dynamic effects of noise colour on a population system that exhibits cycling in the absence of noise. Benton & Beckerman (2005) made several useful observations based on a laboratory soil mite system that help motivate such a study. Population cycling is common: 30% of species in a large database of population dynamics cycled (Kendall *et al.* 1998). Models have suggested that under some conditions, population cycling is an evolutionarily stable state (Greenman *et al.* 2005).

In a controlled experiment, we tested the effects of noise colour on a population with non-equilibrium long-run behaviour and strong interactions between life-stages. In the absence of environmental stochasticity, our system fluctuated at two different frequencies in different experimental treatments. We examined the effects of different colours of noise on population and life-stage means, variances and power spectra (henceforth *spectra*). We tested the predictions of single-species equilibrium theory. We also compared data to theory for multi-species and multi-life-stage systems (e.g. Ripa *et al.* 1998; Ripa & Ives 2003; Xu & Li 2003; Greenman & Benton 2003, 2005a,b).

Flour beetles of the genus *Tribolium* have long been used for studies of population dynamics (Costantino *et al.* 2005). We used the *Tribolium castaneum* laboratory system, which has been accurately modelled (Cushing *et al.* 2003). Our study closely linked new data, analysed here for the first time, with a mechanistic model that allowed detailed descriptions of the effects of noise colour on population spectra. The complete data are in Appendix S3.

Our results show that changes in the colour of environmental noise can change the mean, variability or main periodicity of cycling populations. Noise of one colour shifted the main periodicity of one oscillating population, but noise of another colour did not. Changes in the colour of some weather indices due to anthropogenic change (Wigley *et al.* 1998) can affect industrially exploited populations or pests, disease vectors of public health importance and species' extinction probabilities, so our results have practical significance.

MATERIALS AND METHODS

Model and experiments

We analysed our experiments using the Lattice Stochastic Demographic Larvae–Pupae–Adult (LSD-LPA) model, which has been well tested in constant- and periodic-volume experiments (Costantino *et al.* 1998; Dennis *et al.* 2001; Cushing *et al.* 2003; Reuman *et al.* 2006):

$$L_{t+1} = \mathrm{rd}\left(\left[\sqrt{bA_t \exp\left(-c_{\mathrm{el}}\frac{L_t}{V_t} - c_{\mathrm{ea}}\frac{A_t}{V_t}\right)} + E_{1t}\right]^2\right)$$

$$P_{t+1} = \mathrm{rd}([\sqrt{(1-\mu_{\mathrm{l}})L_t} + E_{2t}]^2)$$

$$A_{t+1} = \mathrm{rd}\left(P_t \exp\left(-c_{\mathrm{pa}}\frac{A_t}{V_t}\right)\right) + \mathrm{rd}((1-\mu_{\mathrm{a}})A_t).$$

Here L_t, P_t and A_t are, respectively, the populations of larvae, pupae and adults at time step t (in units of 2 weeks), V_t is the habitat volume (in units of 20 g) from step t to $t + 1$, [x] denotes the maximum of x and 0, and rd denotes rounding to the nearest integer. Parameter b is fecundity; c_{el}, c_{ea} and c_{pa} quantify cannibalism of eggs by larvae, eggs by adults and pupae by adults, respectively; and μ_{l} and μ_{a} are mortality rates of larvae and adults, respectively. E_{1t} and E_{2t} are bivariate normal random variables with mean zero and covariance matrix $\boldsymbol{\Sigma}$, independent through time. There is no random noise term E_{3t} because the number of adults at each step was controlled. The deterministic skeleton, called the LPA model, is obtained by setting $E_{it} = 0$ and removing rounding.

Our 2×4 factorial experimental design had two population-dynamic regimes and four environmental-noise levels. For dynamic regime 1 (D1), we set $c_{\mathrm{pa}} = 0.0029$ and $\mu_{\mathrm{a}} = 0.3458$; dynamic regime 2 (D2) had $c_{\mathrm{pa}} = 0.53$ and $\mu_{\mathrm{a}} = 0.91$. The adult mortality rate (μ_{a}) was set by removing or adding adults at census time to make the fraction of adults that died during the interval equal to the value specified by D1 or D2. Young adults were added or removed at census time to make the recruitment of new adults consistent with the rate of cannibalism of pupae by adults (c_{pa}) required by D1 or D2.

Coloured environmental stochasticity was generated by changing habitat volume at census time. Four levels of environmental noise were imposed: no noise, with constant habitat size 44 g ($V_t = 44/20 = 2.2$) for all t (three replicates for D1 and three for D2), and red, white and blue noise (five replicates for D1 and five for D2, for each colour). Habitat volume for each noise-affected replicate at each time step randomly took one of the values 8 and 80 g; time series V_t were generated as described in Appendix S1.1. To control for non-spectral properties of noise, spectral mimicry (Cohen *et al.* 1999) was used: each red and blue volume time series V_t

used in D1 was a permutation of a white volume time series also used in D1. Noise time series applied to D2 were matched with each other in the same way, but were independent of time series used in D1. White-noise time series used in D1 were given the 'W-numbers' W1–W5 and matching coloured-noise time series were given the same designations. Noise time series of D2 were assigned the W-numbers W6–W10 in the same way. Population time series of noise-affected replicates were assigned the W-number of their noise. Reddened (respectively, blue-shifted) volume time series had lag-1 autocorrelations of approximately 0.9 (respectively, −0.9). Complete volume time series are in Appendix S3.

Beetles were cultured in 237-mL milk bottles on standard medium (93.5% wheat flour, 5% dried brewers yeast and 1.5% fumagilin-B powder) and kept in a dark incubator at 31 °C (±1°) and 45% relative humidity (±3%). Larvae, pupae and adults were counted and returned to fresh medium every 2 weeks for 80 weeks, giving 36 trivariate population time series of length 41 (the initial condition for each replicate plus one data point per 2 weeks). Initial conditions were $(L_0, P_0, A_0) = (220, 4, 139)$ for all experiments and simulations.

Expected dynamics without noise

Without environmental stochasticity, the system state (L_t, P_t, A_t) was expected to oscillate approximately periodically with period two time steps for D1 and three time steps for D2. These dynamics are among the simplest possible other than equilibrium. For D1, stage distributions were expected to be alternately dominated by larvae and adults, and by pupae and adults. For D2, stage distributions were expected to alternate among larvae-, pupae- and adult-dominated distributions. Expectations were from the LPA model with parameters of Dennis *et al.* (2001).

The intrinsic growth rate, r, of total populations is the (log-scale) asymptotic rate of growth for arbitrarily large V, where cannibalism is negligible. As μ_a was bigger for D2 than for D1 and b and μ_l were the same, D1 had higher r.

Detecting treatment effects with time-series statistics and ANOVA

To detect effects of dynamic regimes and noise colours on population dynamics for tests of theoretical predictions, statistical descriptors were computed from each experimental replicate's time series, and ANOVAs were carried out with dynamic regimes and noise colours as predictors and the statistics as response variables.

Time-series statistics

The total population of a replicate at time t was $L_t + P_t + A_t$. For each experimental replicate, the mean and variance over all time steps including the initial condition of the L-, P- and A-stages and the total population were calculated. The correlation coefficient, R, between total population and V_t was calculated for each replicate after discarding the initial total population. Log powers at normalized frequency (nf) 0 and 1 were computed for L-, P- and A-stages and total populations. The nf is in units of cycles per 4 weeks. To convert nf to period in weeks, divide 4 by nf. Increased power at nf 0 is spectral reddening; increased power at nf 1 is blue shifting (Cohen 1995). Linear combinations of autocorrelations of different lags were computed for L-, P- and A-stages and total populations of each replicate.

ANOVA

Because noise time series were matched by W-number across the noisy treatments of D1 (respectively, D2), the values of any statistic on population time series with the same W-number were not independent. To account for this dependence, linear models for ANOVAs included a random effect for W-number that captured effects of the composition of the white-noise time series of which matched coloured-noise time series were permutations.

For each time-series statistic as the response variable, a linear model with fixed effects for noise colour, dynamics and the interaction, and a random effect for W-number was fitted (Pinheiro & Bates 2000). It was not practical to consider higher-level interactions due to limited replication. Starting from this model, F-tests were used to test whether: (i) the interaction effect was significant, (ii) noise colour had a significant effect within D1, (iii) noise colour had a significant effect within D2 and (iv) dynamical regime had a significant effect within each noise colour level, separately. Standard one-way ANOVAs were used to detect significant effects of dynamics regime between the no-noise treatments. No ANOVA used both control and treatment data, which had different replication, so all designs were balanced.

For all linear models, homogeneity of residual variance across treatments was not rejected (Levene's test, 1% level). Normality of predicted random effects, if present, was never rejected (Shapiro–Wilk test, 1% level). While normality of residual distributions was rejected for 2 of the 60 models considered (Shapiro–Wilk, 1%), these distributions did not differ radically from normal when inspected visually. As ANOVA using balanced data is robust to departures from normality, departures were not considered important, but were reported.

Detecting and describing treatment effects using a dynamical model

To provide a detailed picture of how noise colour affected population cycling, the LSD-LPA model was parameterized

and then used with a *spectrum enhancement method* of Reuman *et al.* (2006).

Model fitting and validation

Following Dennis *et al.* (2001) and Cushing *et al.* (2003), the LSD-LPA model was fitted to data by conditional least squares (CLS; Appendix S1.2). Using the best parameters to generate time series from the model, the power spectra of the data and model simulations were compared. A good agreement was a validation of the model. Two tests of Reuman *et al.* (2006) give *P*-values describing the frequency-domain fit of a stochastic model with time-series data. The *spectrum distance fit test* indicates a good fit if the data log spectrum is closer to the mean model log spectrum across all frequencies than a large enough percentage of model log spectra from individual simulations. The *spectrum shape fit test* indicates a good fit if the data log spectrum has shape more similar to that of the mean model log spectrum than a large enough number of model log spectra from individual simulations. These methods were modified to give a single *P*-value per experimental treatment, rather than one per replicate (Appendix S1.3). Another technique, similar to techniques applied previously (Tsay 1992; Cohen 1995; Stenseth *et al.* 1996; Grenfell *et al.* 2002), provided a visual indication of fit. A good time-domain fit did not necessarily imply a good frequency domain fit, nor vice versa (Reuman *et al.* 2006).

The LSD-LPA model was also validated using the 'probe-matching' methods of Kendall *et al.* (1999) and others, by which distributions of a statistic computed from model-generated time series are compared with values of the statistic for time series from an experimental treatment (Appendix S1.4). Statistics described above (see Time-series statistics) were used.

Using the model to distinguish noise-colour effects

To study treatment effects, time series output of the LSD-LPA model with c_{pa}, μ_a and noise corresponding to experimental treatment i was compared with data from experimental treatment j for $i \neq j$. This was called *cross-comparison* of the model with data. Frequency-domain cross-comparison was performed via the spectrum distance and shape fit tests and using visual spectral comparison. Probe-matching cross-comparisons were also performed.

Some cross-comparisons were carried out between a model and data with the same c_{pa} and μ_a values (i.e. both were from D1 or both were from D2) but affected by different noise factor levels, h and k. If cross-comparison rejected the null hypothesis that data from noise level h came from the model with noise level k, and rejected the null hypothesis that data from noise level k came from the model with noise level h, then cross-comparison demonstrated a statistically significant noise-colour effect.

Model validation and cross-comparison differed only according to whether $i = j$ or $i \neq j$. The combination of validation and cross-comparison involved 64 comparisons in an 8 by 8 matrix format with $8 = 2 \times 4$ factorial experimental treatments along the columns and corresponding 'model treatments' along the rows. Validation and cross-comparison were sometimes carried out together, and results were presented in matrix format with validation along the diagonal. Validation and cross-comparison for treatments within D1 or D2 were sometimes presented in a 4 by 4 matrix format.

Describing treatment effects with the spectrum enhancement method

Spectral estimates from length-41 time series lack resolution. The spectrum enhancement method of Reuman *et al.* (2006) allowed inferences about detailed properties of population spectra and the effects of noise colour on spectra (and therefore on dynamics) by combining data from short time series and a mechanistic dynamical model. To make high-resolution predictions, we generated many time series of length 1024 using the fitted and validated LSD-LPA model. Spectral estimates based on these time series were model-based hypotheses of population spectra under different noise-colour regimes. They provided a comprehensive, high-resolution prediction of the most important spectral effects of noise colour on dynamics and allowed the identification of appropriate statistics to detect these effects in data.

The spectrum enhancement predictions were validated by calculating from the data a difference of autocorrelation statistics of different lags. In this way, our results do not depend on spectral enhancement, although spectral enhancement was used to suggest statistical indicators that could detect them.

RESULTS

Some time series are shown in Fig. 1. We first present ANOVA results of time-series statistics to test single-species theory and demonstrate significant dynamics–noise colour interactions; we then use the LSD-LPA model and the spectrum enhancement method to describe these interactions in detail; and finally we validate spectrum-enhancement results with data.

Tests of single-species theory using time-series statistics and ANOVA

Population tracking of noise

Consistent with prediction (1) of the Introduction, for both dynamical regimes, the correlation coefficient R between total population and habitat volume was on average highest for red noise, lowest for blue noise and intermediate for

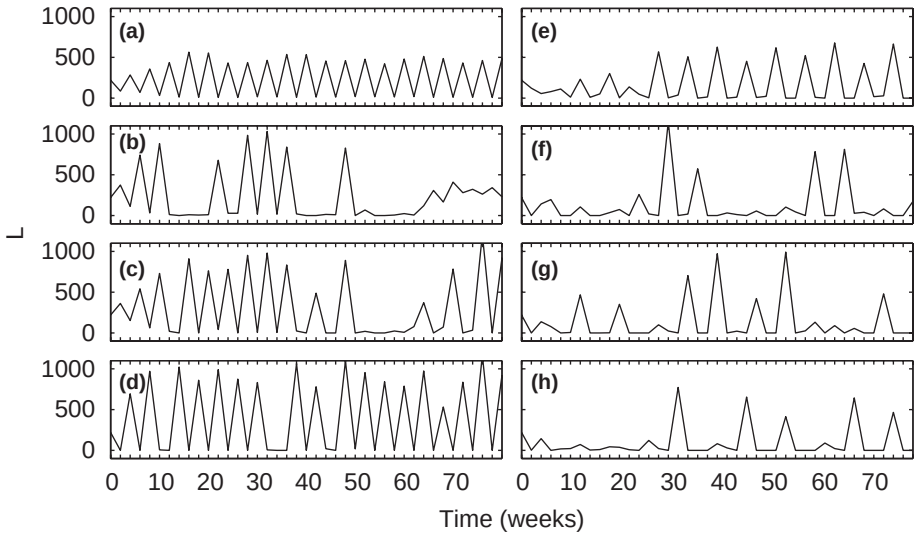

Figure 1 The larval stage of one representative replicate from each experimental treatment: no noise (a, e); red noise (b, f); white noise (c, g); blue noise (d, h); dynamic regime D1 (a–d) and dynamic regime D2 (e–h). Time series in panels (b–d) (respectively, f–h) have the same W-number (Materials and methods). Other life stages and volume time series for the same replicates are in Fig. S1. Other replicates are in Appendix S3.

white noise. It was positive for all replicates. Differences between noise treatments were significant (Table 1). Consistent with prediction (2), for each noise factor level, R was on average higher for the high-r regime D1 than for the low-r regime D2. Differences were significant ($P < 0.0001$ for red, white and blue noise, separately).

Population spectra are tinged by coloured noise

Consistent with prediction (3), spectra of total populations and some life stages were somewhat reddened when the environment varied by red noise. For the L and P stages and for the total population, log power at nf 0 was on average highest for red noise, intermediate for white noise and lowest for blue noise treatments for both dynamic regimes. Differences were significant or marginally so (Table 1). Mean log power at nf 0 for the A stage was not significantly different among noise treatments for either D1 or D2 (Table S1D).

For D1, spectra of total populations and all life stages were tinged blue by blue noise: log power at nf 1 was on

Table 1 Summary statistics for experimental data

Dynamics treatment	No noise	Red noise	White noise	Blue noise	ANOVA, three noisy treatments
(A) Noise-tot. pop. R					
D1	NA	0.841	0.687	0.624	< 0.0001
D2	NA	0.684	0.388	0.287	< 0.0001
(B) Log power, nf 0, L					
D1	2.52	4.35	4.01	3.50	0.0001
D2	3.28	4.01	3.73	3.50	0.0245
(C) Log power, nf 1, L					
D1	4.63	4.71	4.77	5.10	0.0011
D2	3.10	3.74	3.86	3.76	0.4273
(D) Var. total pop.					
D1	30 216	338 438	268 140	232 665	0.0042
D2	29 993	107 645	80 438	59 725	0.2838

Columns 2–5 show means over replicates within each treatment of values computed for each replicate: (A) correlation R between total population (starting with $t = 2$) and flour volume V since the previous time step; (B) log power at normalized frequency (nf) 0, larval (L) life stage; (C) log power at nf 1, L life stage and (D) variance of total population. Column 6 shows the P-value significance of noise colour effects within D1 and D2 separately. No violations of linear model assumptions occurred (Materials and methods).

average highest for blue noise, intermediate for white noise and lowest for red noise treatments (L-stage, Table 1; others Table S1D). For D2, there was no significant association of noise colour with log power at nf 1 for any life stage.

These results support the hypothesis that, under some dynamic regimes, spectra of total populations and of life stages partially reflect the colour of the spectra of noise. However, power at nf 0 and 1 describes only the extremes of the spectrum. We demonstrated only that this small part can be affected by coloured noise as hypothesized. We will show that the effects of coloured noise on the whole spectrum are complex. Red noise did not lead to reddened population spectra if reddened population spectra were understood to decrease monotonically or nearly so with increasing frequency (see Spectrum enhancement results below).

Variability of total population

Consistent with prediction (4), among treatments affected by noise, variances of total populations were on average highest for red noise and lowest for blue noise for both D1 and D2. Differences were significant for D1 but not for D2 (Table 1). Variances of total populations were higher on average in the presence of any colour of environmental stochasticity than in its absence.

Consistent with prediction (5), populations of high r were more variable in non-constant environments than populations of low r. For all treatments affected by noise, variances of total populations were on average higher for D1 than for D2 and differences were significant ($P < 0.0001$ for red, white and blue, separately). In a constant environment, contrary to prediction (6), variances of total populations were not significantly different between D1 and D2 (ANOVA, $P = 0.933$).

Dynamics and noise colour interacted

Mean total populations increased from the red to white to blue noise treatments in D1, but decreased for the same progression in D2. This interaction between noise colour and dynamics was statistically significant (Fig. 2a). For D1, mean total populations were less for red noise than for no noise, but were larger for white noise than for no noise and still larger for blue noise. For D2, populations were reduced, relative to no environmental noise, in the presence of noise of all colours, most by blue noise and least by red noise (Table S1A). L- and P-stage mean populations followed the same pattern and A-stage populations followed a similar pattern (Fig. 2b; Table S1A).

For D1, among treatments affected by noise, L-stage variances were on average highest for blue noise and lowest for red noise; for D2, the reverse pattern held. This interaction effect was statistically significant (Fig. 2c).

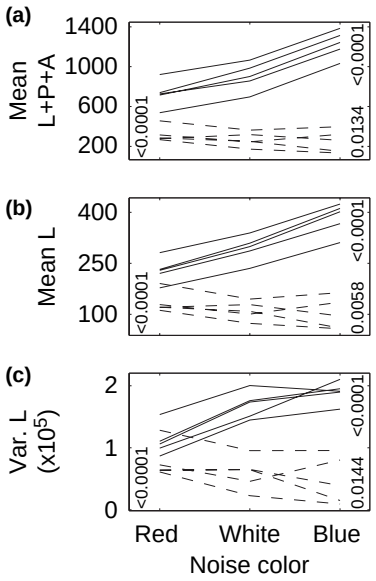

Figure 2 Interaction effects between intrinsic dynamics and noise colour on mean total population (a), mean larval (L) population (b) and the variance of L over time (c). Replicates matched by spectral mimicry are connected (Materials and methods): solid lines are for dynamic regime D1 ($c_{pa} = 0.0029$, $\mu_a = 0.3458$); dashed lines are for D2 ($c_{pa} = 0.53$, $\mu_a = 0.91$). P-values (Materials and methods) on the left of each panel are for interaction effects; in the upper right are for the effects of noise colour on D1; and in the lower right are for the effects of noise colour on D2.

P-stage variances showed the same pattern. Although variances of L-stage populations were comparable between D1 and D2 in the absence of environmental stochasticity, D1 L-stage variances were much higher than D2 variances for treatments affected by noise of the same colour (Table S1B). Significant interactions were also observed using other statistics (Table S1).

Interactions between noise colour and dynamics inferred using a dynamical model

The LSD-LPA model and the spectrum enhancement method illuminated the observed interactions between nonlinear dynamics and noise colour.

Model fitting and validation

CLS best-fitting parameters of the LSD-LPA model were similar to but not the same as those obtained by the same methods for a previous experiment in constant habitat volume (Table S2). With Table S2 parameters, the LSD-LPA model fitted data in the frequency domain, visually and using the spectrum distance and shape fit tests (Fig. 3a). The LSD-LPA model was also validated using the mean total population statistic (Fig. 3b), the mean L-stage population

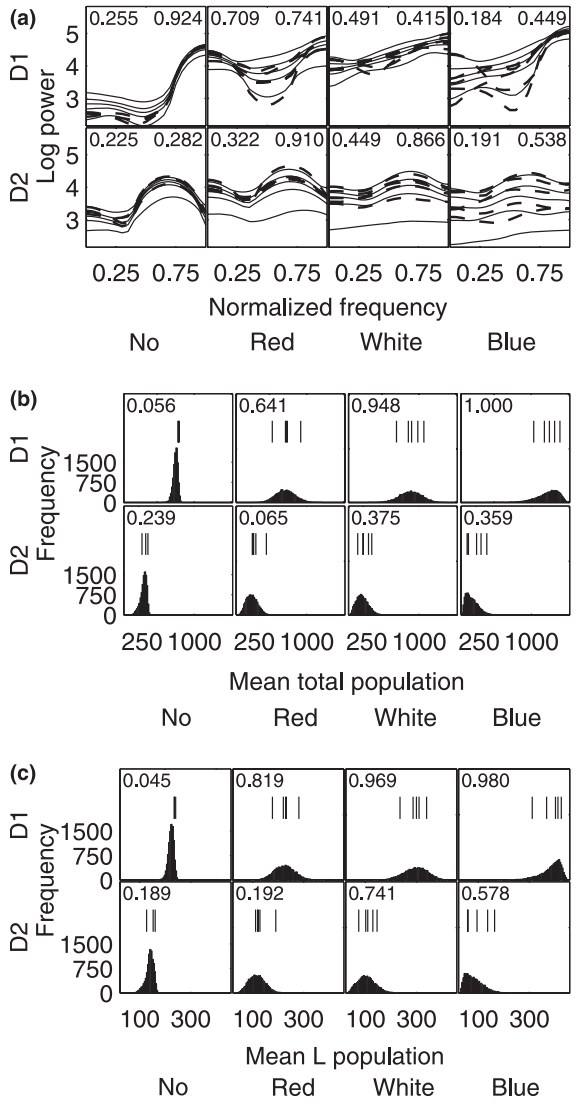

Figure 3 Validation of the LSD-LPA model with parameters of Table S2. Panels in each plot have rows corresponding to dynamic regime D1 and D2 and columns corresponding to the four noise factor levels, as shown to the left and below the axis labels. (a) Thick dashed lines are log spectra of experimental data, L-stage. Thin solid lines are 2.5th, 25th, 50th, 75th and 97.5th percentiles of log-spectra of the L-stage of 10 000 model-generated time series of the same length as the data, showing the distribution of possible model spectra. *P*-values in the corners of each panel are from the spectrum distance (upper left) and spectrum shape (upper right) fit tests. Visual comparisons for other life stages are in Figs. S3; *P*-values here reflect the fit of all life stages. Histograms are distributions of mean total populations (b) and mean L populations (c) from 10 000 model-generated time series of the same length as the data. Vertical lines, one for each experimental replicate, are data mean total populations (b) and data mean L populations (c). Numbers in each panel are *P*-values for a test of the null hypothesis that data and model distributions are the same (Materials and methods).

statistic (Fig. 3c), the other mean life-stage population statistics, variances of total populations and life stages, and other statistics (Fig. S4). The LSD-LPA model was an excellent description of the study system.

Using fitted parameter values, the intrinsic growth rate r was $\log_{10}(2.266) = 0.3553$ for D1, 13.7% higher than the D2 value, $\log_{10}(2.053) = 0.3124$. 10^r is the dominant eigenvalue of the deterministic transition equations (Model and experiments) in the limit of large V. It is the asymptotic factor by which the population stage vector is multiplied at each time step in the absence of density dependence; hence r has dimensions of inverse time.

Spectrum enhancement results

Spectral predictions of the LSD-LPA model using the spectrum enhancement method predicted detailed noise-colour effects (Fig. 4). Features of the spectra in Fig. 4 that are not visible in Fig. 3a are model-based predictions that provide a framework for understanding noise–dynamics interactions and will guide further data analysis.

Red environmental noise increased power at very low frequencies (Fig. 4, comparing the left sides of the panels across each row). However, spectral tingeing by the colour of environmental noise does not explain the effects of noise at other frequencies, which are dominant. Spectra are not well-characterized as reddened or blue-shifted,

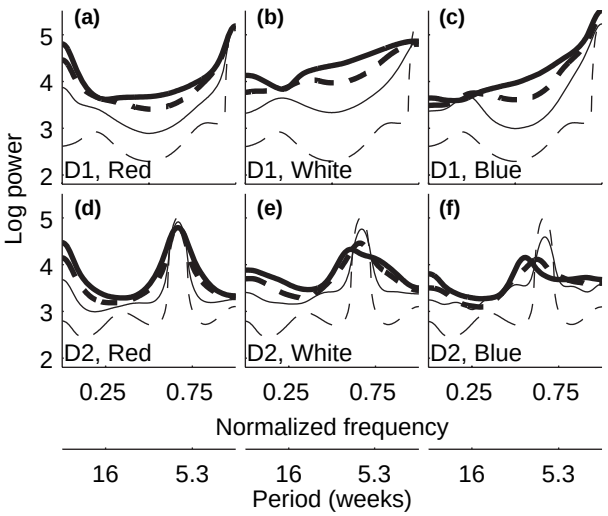

Figure 4 Predicted detailed log spectra using the LSD-LPA model, L-stage. Thin dashed lines on each plot correspond to no imposed environmental noise (the controls). Thick solid lines correspond to experimentally imposed noise (V oscillating stochastically between 80 and 8 g). Thick dashed lines correspond to moderate environmental noise ($V = 68$ or 20 g) and thin solid lines correspond to weak noise ($V = 56$ and 32 g). Log spectra shown are means of 500 log spectra of model-generated time series of length 1024. Other life stages are in Fig. S5.

even for treatments affected by red and blue noise, respectively.

The effects of coloured noise on population spectra were complex (Fig. 4). As expected, experimental populations in constant-volume habitats oscillated approximately periodically with period about two time steps for D1 and three time steps for D2. This oscillation was visible in experimental data (Fig. 1a,e) and was reflected in the main peaks of the spectra (thin dashed lines, Fig. 4) of treatments with no environmental noise at nf 1 for D1 and nf 0.66 for D2. For D2, blue and white noise shifted the main frequency of population oscillation towards lower frequencies, but red noise did not. D2 populations oscillated with period approximately four time steps when affected by blue noise. In contrast, for D1, the main spectral peak was not shifted by noise of any colour, although its prominence was affected differently by noise of different colours (Fig. 4a–c). The effects of noise colour for D1 were distributed across the frequency range, whereas, for D2, only the main spectral peak and low frequencies were substantially changed.

Validation of model predictions

The spectrum distance and shape fit tests measure how spectra differ at all frequencies, weighted equally. As the predicted spectral differences among noise colours for D1 were distributed across the frequency range, the spectrum distance and shape fit tests were used to cross-compare noise treatments. Cross-comparison revealed statistically significant effects of noise colour on population spectra, validating predictions of spectrum enhancement (Fig. 5a).

Population variance is the integral of the spectrum. As D1 L-stage spectra differed by noise colour across the whole frequency range, not surprisingly L-stage variance was affected by noise colour: ANOVA showed statistical significance of the effect ($P < 0.0001$; Fig. 2c). Cross-comparison using the L-stage variance statistic (Fig. S4) confirmed significance.

The most noticeable predicted effect of noise colour on D2 was the shift of the main period of population oscillation from three to four time steps. The statistic, $R(4)–R(3)$, equal to the lag-4 autocorrelation minus the lag-3 autocorrelation of a life-stage, was used to assess the empirical amount and statistical significance of this predicted shift. Cross-comparison using this statistic and the L, P and A stages demonstrated statistically significant effects of noise colour on the main period of oscillation of the *T. castaneum* system (Fig. 5b, Fig. S4). ANOVA applied to $R(4)–R(3)$ for noise-affected D2 replicates also showed significance (e.g. $P = 0.0022$ for the L-stage; Table S1C), validating spectrum enhancement predictions.

DISCUSSION

Our results show that noise colour can substantially affect the dynamics of a cycling population. The principal periodicity of one population differed by 33% under different noise colours. Noise colour also affected population means and variances. Colour effects depended on the details of dynamics without noise: effects were often opposite for different types of population cycling. These results have practical and theoretical implications.

Practical implications

Extinction

Modelling studies have found both increased and decreased extinction risk under reddened environmental noise relative to white noise (Petchey *et al.* 1997; Morales 1999; Schwager *et al.* 2006). We showed that population means and variances can be larger or smaller under red noise than under white noise, depending on deterministic dynamics. Means and variances are related to extinction risks, so it is not surprising that extinction risk is related to noise colour in a complex way, and that prior results have been non-uniform. A body of theoretical literature, including Greenman & Benton (2003, 2005a,b) and Ripa & Ives (2003), has begun to recognize and explore the complexity of the noise colour–extinction risk relationship, but more theoretical and experimental work would be useful, especially for cycling populations.

Climate change

Human-induced climate change includes changes in the colour of weather-index fluctuations for indices such as temperature (Wigley *et al.* 1998). Petchey (2000) predicted that such changes would affect population dynamics. Gonzalez & Holt (2002) argued that changes in the colour of environmental spectra can affect source-sink population dynamics and the frequency of outbreaks of rare species at range margins. Fontaine & Gonzalez (2005) demonstrated that regional synchronization of fluctuating populations, which affects metapopulation extinction risk, is influenced by environmental noise colour. Our result that changes in environmental noise colour can modify the periodicity of cycling populations adds another reason why future studies of the impacts of climate change should quantify not only the impacts of changing weather averages and variability, but also the impacts of changing colour. It will be important to determine appropriate weather indices on which vital rates of individuals within populations depend as well as appropriate time scales on which the environment affects these rates in order to choose appropriate indices and time scales for estimating the effects of changing noise colour (Hallett *et al.* 2004).

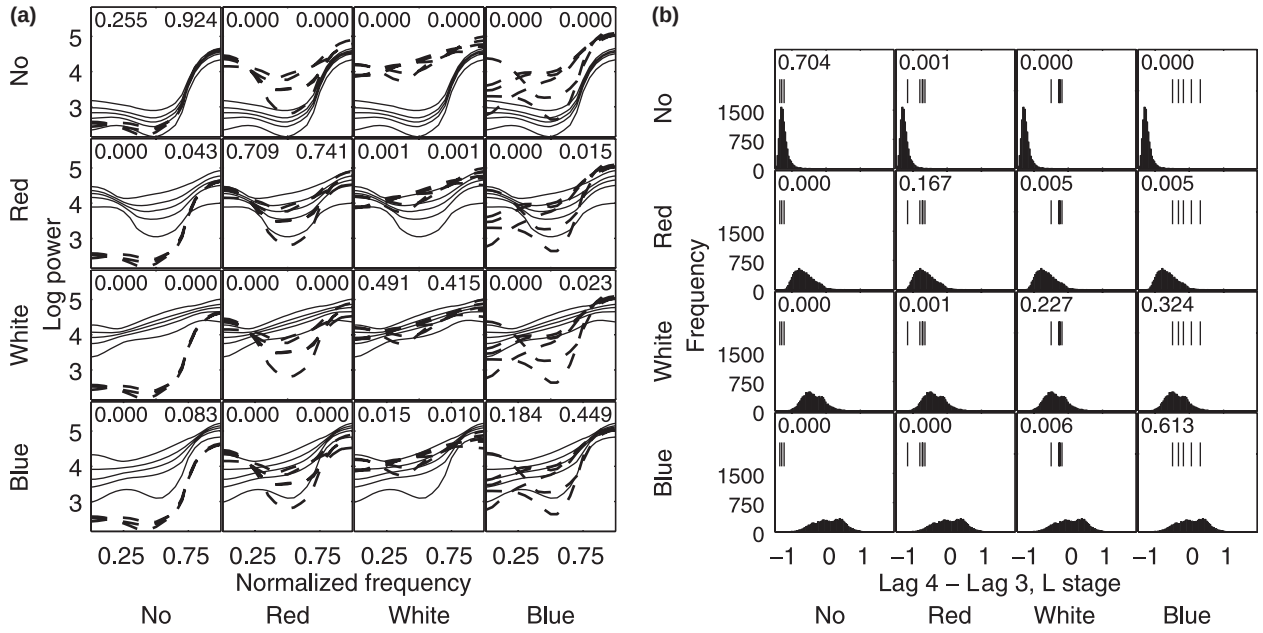

Figure 5 Cross-comparisons show effects of noise colour. (a) Thick dashed lines are log spectra of experimental L-stage time series and are the same in all panels in a column. Each column corresponds to an experimental noise factor level, indicated in capital letters below the column. Thin solid lines show distributions of log-spectra of L-stage LSD-LPA-model-generated time series (Fig. 3a caption) and are the same in all panels in a row. Each row is from model output with noise imposed as indicated to the left of the row. Dynamics were D1. *P*-values in the corners of each panel are from the spectrum distance (upper left) and spectrum shape (upper right) fit tests; they reflect fit for all life stages. Visual spectral cross-comparisons for other life stages are in Fig. S3. (b) As in (a), columns correspond to experimental noise factor levels and rows to noise imposed on the LSD-LPA model. Dynamics were D2. Histograms show distributions of lag-4 autocorrelations minus lag-3 autocorrelations [$R(4) - R(3)$] of the L-stage of 10 000 model-generated time series of the same length as data. Vertical lines, one for each experimental replicate, are the same statistic for data. *P*-values are for a test of the null hypothesis that data and model distributions are the same (Materials and methods). Low *P*-values in off-diagonal panels reflect significant effects of noise colour. Cross-comparisons using $R(4) - R(3)$ for other life stages are in Fig. S4.

Population predictions using models

A better predictive understanding of population dynamics would improve strategies for pest management, sustainable exploitation of resources, climate change mitigation and population viability analyses (Boyce 1992). Our results show that the predictions (1)–(5) may often be useful for making low-resolution predictions about the possible effects of climate change on the dynamics of cycling populations. For specific, quantitative predictions such as viability analyses, our results highlight some lessons that may help researchers construct and apply mechanistic models of field populations given available data. Population models should not assume independent, identically distributed errors over time if noise is expected to have an environmental component. Fitting such models to systems under reddened stochasticity leads to systematic errors (Ranta *et al.* 2000; Jonzén *et al.* 2002). If appropriate environmental covariates were not measured, it may be beneficial to fit population models that include parameters about the external noise such as its autocorrelation, so characteristics of the biologically relevant components of noise can be inferred from population data. As the spectra of environmental fluctuations are changing, population predictions and viability analyses based on model simulations should incorporate estimates of future means, variances and colours of dynamically important weather variables.

Theoretical implications

We showed that many predictions of theory originally intended for a single-stage population that equilibrates without noise also held for stage-structured populations that oscillated without noise. A few predictions of the theory were not supported. For instance, contrary to prediction (6), in a constant environment, high-*r* and low-*r* populations had statistically the same variance, perhaps because *r* for D1 was only 13.7% higher than *r* for D2. However, (6) was also not supported by the results of Petchey (2000) and Laakso *et al.* (2003b).

More crucially, single-species theory lacks detailed predictions of the effects of coloured noise on population spectra. Much debate has centred on why and to what degree

populations and models exhibit 'reddened' or 'blue-shifted' dynamics (Pimm & Redfearn 1988; Cohen 1995; Sugihara 1995; White *et al.* 1996; Kaitala & Ranta 1996; Greenman and Benton 2005a,b). But these terms are qualitative, and cannot adequately describe spectra of complex population systems. Simple quantitative indices such as the spectral exponent can also be insufficient descriptors. The spectral exponent assumes a power-law spectrum, an assumption rarely tested statistically (Inchausti & Halley 2002; Laakso *et al.* 2003a) and one that does not describe *Tribolium* or other oscillating systems (Fig. 4; Bjørnstad *et al.* 2004; Greenman and Benton 2005a,b). It may be easier to identify the dominant ecological causes of common population-spectral characteristics if the broad concept of reddening is amplified by specific spectral characteristics (e.g. Greenman & Benton 2005a,b).

The effects of noise colour on *Tribolium* spectra were more complicated than the predictions of single-species theory. A linear theory predicts the effects of coloured noise on the spectra of complex systems (e.g. Ripa *et al.* 1998; Ripa & Ives 2003; Greenman & Benton 2005a,b), but that theory does not predict changes in the main periodicity of a cycling population (such as those observed here for D2) if that main periodicity comes from underlying deterministic dynamics (Reuman *et al.* 2006). The questions of how common are noise- or noise-colour-induced shifts in main population periodicities, and how accurate the multi-stage theory is generally for cycling populations, are important and unanswered.

ACKNOWLEDGEMENTS

The authors thank Tim Coulson, Tim Benton, Owen Petchey and an anonymous referee for helpful comments and Priscilla Rogerson for assistance. JEC thanks W.T. Golden and family for hospitality and dedicates his contribution to honour the memory of W.T. Golden. The authors were supported by US National Science Foundation grant DMS 0443803. The contribution of DCR was partly supported by his participation in a UK NERC working group, grant NE/C514474/1, and an NCEAS working group on unifying methods of inference in ecology.

REFERENCES

Ariño, A. & Pimm, S.L. (1995). On the nature of population extremes. *Evol. Ecol.*, 9, 429–443.

Benton, T.G. & Beckerman, A.P. (2005). Population dynamics in a noisy world: lessons from a mite experimental system. *Adv. Ecol. Res.*, 37, 143–181.

Bjørnstad, O.N., Nisbet, R.M. & Fromentin, J.-M. (2004). Trends and cohort resonance effects in age-structured populations. *J. Anim. Ecol.*, 73, 1157–1167.

Boyce, M.S. (1992). Population viability analysis. *Annu. Rev. Ecol. Syst.*, 23, 481–506.

Cohen, J.E. (1995). Unexpected dominance of high frequencies in chaotic nonlinear population models. *Nature*, 378, 610–612.

Cohen, J.E., Newman, C.M., Cohen, A.E., Petchey, O.L. & Gonzalez, A. (1999). Spectral mimicry: a method of synthesizing matching time series with different Fourier spectra. *Circuits Syst. Signal Process*, 18, 431–442.

Costantino, R.F., Cushing, J.M., Dennis, B., Desharnais, R.A. & Henson, S.M. (1998). Resonant population cycles in temporally fluctuating habitats. *Bull. Math. Biol.*, 60, 247–273.

Costantino, R.F., Desharnais, R.A., Cushing, J.M., Dennis, B., Henson, S.M. & King, A.A. (2005). Nonlinear stochastic population dynamics: the flour beetle *Tribolium* as an effective tool of discovery. *Adv. Ecol. Res.*, 37, 101–141.

Cushing, J.M., Costantino, R.F., Dennis, B., Desharnais, R.A. & Henson, S.M. (2003). *Chaos in Ecology: Experimental Non-linear Dynamics*. Academic Press, New York.

Dennis, B., Desharnais, R.A., Cushing, J.M., Henson, S.M. & Costantino, R.F. (2001). Estimating chaos and complex dynamics in an insect population. *Ecol. Monogr.*, 71, 277–303.

Fontaine, C. & Gonzalez, A. (2005). Population synchrony induced by resource fluctuations and dispersal in an aquatic microcosm. *Ecology*, 86, 1463–1471.

Gonzalez, A. & Holt, R.D. (2002). The inflationary effects of environmental fluctuations in source-sink systems. *Proc. Natl Acad. Sci. U.S.A.*, 99, 14872–14877.

Greenman, J.V. & Benton, T.G. (2003). The amplification of environmental noise in population models: causes and consequences. *Am. Nat.*, 161, 225–239.

Greenman, J.V. & Benton, T.G. (2005a). The frequency spectrum of structured discrete-time population models: its properties and their ecological implications. *Oikos*, 110, 369–389.

Greenman, J.V. & Benton, T.G. (2005b). The impact of environmental fluctuations on structured discrete time population models: resonance, synchrony and threshold behavior. *Theor. Popul. Biol.*, 68, 217–235.

Greenman, J.V., Benton, T.G., Boots, M. & White, A.R. (2005). The evolution of oscillatory behavior in age-structured species. *Am. Nat.*, 166, 68–78.

Grenfell, B.T., Bjørnstad, O.N. & Finkenstädt, B.F. (2002). Dynamics of measles epidemics: scaling noise, determinism, and predictability with the TSIR model. *Ecol. Monogr.*, 72, 185–202.

Hallett, T.B., Coulson, T.N., Pilkington, J.G., Clutton-Brock, T.H., Pemberton, J.M. & Grenfell, B.T. (2004). Why large-scale climate indices seem to predict ecological processes better than local weather. *Nature*, 430, 71–75.

Inchausti, P. & Halley, J.M. (2002). The long-term variability and spectral colour of animal populations. *Evol. Ecol. Res.*, 4, 1–16.

Jillson, D.A. (1980). Insect populations respond to fluctuating environments. *Nature*, 288, 699–700.

Jonzén, N., Lundberg, P., Ranta, E. & Kaitala, V. (2002). The irreducible uncertainty of the demography-environment interaction in ecology. *Proc. R. Soc. Lond., B, Biol. Sci.*, 269, 221–225.

Kaitala, V. & Ranta, E. (1996). Red/blue chaotic power spectra. *Nature*, 381, 198–199.

Kaitala, V., Ylikarjula, J., Ranta, E. & Lundberg, P. (1997). Population dynamics and the color of environmental noise. *Proc. R. Soc. Lond., B, Biol. Sci.*, 264, 943–948.

Kendall, B.E., Prendergast, J. & Bjørnstad, O.N. (1998). The macroecology of population dynamics: taxonomic and biogeographic patterns in population cycles. *Ecol. Lett.*, 1, 160–164.

Kendall, B.E., Briggs, C.J., Murdoch, W.M., Turchin, P., Ellner, S.P., McCauley, E. *et al.* (1999). Why do populations cycle? A synthesis of statistical and mechanistic modeling approaches. *Ecology*, 80, 1789–1805.

Laakso, J., Kaitala, V. & Ranta, E. (2001). How does environmental variation translate into biological processes? *Oikos*, 92, 119–122.

Laakso, J., Kaitala, V. & Ranta, E. (2003a). Non-linear biological responses to disturbance: consequences on population dynamics. *Ecol. Modell.*, 162, 247–258.

Laakso, J., Löytynoja, K. & Kaitala, V. (2003b). Environmental noise and population dynamics of the ciliated protozoa *Tetrahymena thermophila* in aquatic microcosms. *Oikos*, 102, 663–671.

Luckinbill, L.S. & Fenton, M.M. (1978). Regulation and environmental variability in experimental populations of protozoa. *Ecology*, 59, 1271–1276.

May, R.M. (1973). *Stability and Complexity in Model Ecosystems*. Princeton University Press, Princeton.

May, R.M. (1981). Models for single populations. In: *Theoretical Ecology: Principles and Applications* 2nd edn. pp. 5-29. (ed. May, R.M.). Blackwell Scientific, Oxford.

Morales, J.M. (1999). Viability in a pink environment: why "white noise" models can be dangerous. *Ecol. Lett.*, 2, 228–232.

Nisbet, R.M. & Gurney, W.S.C. (1982). *Modeling Fluctuating Populations*. Wiley, Chichester.

Nisbet, R.M., Gurney, W.S.C. & Pettipher, M.A. (1977). An evaluation of linear models of population fluctuations. *J. Theor. Biol.*, 68, 143–160.

Petchey, O.L. (2000). Environmental color affects aspects of single-species population dynamics. *Proc. R. Soc. Lond., B, Biol. Sci.*, 267, 747–754.

Petchey, O.L., Gonzalez, A. & Wilson, H.B. (1997). Effects on population persistence: the interaction between environmental noise color, intraspecific competition and space. *Proc. R. Soc. Lond., B, Biol. Sci.*, 264, 1841–1847.

Pimm, S. & Redfearn, A. (1988). The variability of population densities. *Nature*, 334, 613–614.

Pinheiro, J.C. & Bates, D.M. (2000). *Mixed-Effects Models in S and S-Plus*. Springer, New York.

Ranta, E., Lundberg, P., Kaitala, V. & Laakso, J. (2000). Visibility of the environmental noise modulating population dynamics. *Proc. R. Soc. Lond., B, Biol. Sci.*, 267, 1851–1856.

Reuman, D.C., Desharnais, R.A., Costantino, R.F., Ahmad, O.S. & Cohen, J.E. (2006). Power spectra reveal the influence of stochasticity on nonlinear population dynamics. *Proc. Natl Acad. Sci. U.S.A.*, 103, 18860–18865.

Ripa, J. & Ives, A.R. (2003). Food web dynamics and autocorrelated environments. *Theor. Popul. Biol.*, 64, 369–384.

Ripa, J., Lundberg, P. & Kaitala, V. (1998). A general theory of environmental noise in ecological food webs. *Amer. Nat*, 151, 256–263.

Roughgarden, J. (1975). A simple model for population dynamics in stochastic environments. *Amer. Nat*, 109, 713–736.

Schwager, M., Johst, K. & Jeltsch, F. (2006). Does red noise increase or decrease extinction risk? Single extreme events versus series of unfavorable conditions. *Amer. Nat*, 167, 879–888.

Stenseth, N.C., Bjørnstad, O.N. & Saitoh, T. (1996). A gradient from stable to cyclic populations of *Clethrionomys rufocanus* in Hokkaido, Japan. *Proc. R. Soc. Lond., B, Biol. Sci.*, 263, 1117–1126.

Sugihara, G. (1995). From out of the blue. *Nature*, 378, 559–560.

Tsay, R.S. (1992). Model checking via parametric bootstraps in time series analysis. *Appl. Statist*, 41, 1–15.

Vasseur, D.A. & Yodzis, P. (2004). The color of environmental noise. *Ecology*, 85, 1146–1152.

White, A., Bowers, R.G. & Begon, M. (1996). Red/blue chaotic power spectra. *Nature*, 381, 198.

Wigley, T.M.L., Smith, R.L. & Santer, B.D. (1998). Anthropogenic influence on the autocorrelation structure of hemispheric-mean temperatures. *Science*, 282, 1676–1679.

Xu, C.-L. & Li, Z.-Z. (2003). Population dynamics and the color of environmental noise: a study on a three-species food chain system. *Ecol. Res.*, 18, 145–154.

SUPPLEMENTARY MATERIAL

The following supplementary material is available for this article:

Figure S1 One time series from each experimental replicate.
Figure S2 Bootstrapped conditional least squares parameter estimates.
Figure S3 Frequency domain validation and cross-comparison.
Figure S4 Validation and cross-comparison with time-series statistics.
Figure S5 Spectrum enhancement method results.
Table S1 Summary statistics for experimental data.
Table S2 Fitted model parameters and parameters of Dennis *et al.* (2001).
Appendix S1 Additional methods.
Appendix S2 Supporting results.
Appendix S3 Complete experimental data.

This material is available as part of the online article from: http://www.blackwell-synergy.com/doi/full/10.1111/j.1461-0248.2008.01194.x

Please note: Blackwell Publishing are not responsible for the content or functionality of any supplementary materials supplied by the authors. Any queries (other than missing material) should be directed to the corresponding author for the article.

Editor, Gregor Fussmann
Manuscript received 19 February 2008
Manuscript accepted 24 March 2008

Appendix S1: Additional Methods

Appendix S1.1: Habitat volume time series

The colored time series V_t were generated for D1 and D2 separately as follows:

1) Generate a 40 by 5 matrix W_1 whose entries are independent and identically distributed (iid) standard normal (i.e., mean 0, standard deviation 1).
2) Generate a 40 by 5 matrix R_2 whose columns are generated using the autoregressive process $x_{t+1} = \rho x_t + \sqrt{1-\rho^2}\,\varepsilon_t$, where ρ = 0.9, and x_0 and ε_t are iid standard normal.
3) Generate a 40 by 5 matrix B_2 whose columns are generated using the same autoregressive process with ρ = -0.9.
4) Apply the spectral mimicry algorithm (Cohen *et al.* 1999) to permute the entries of each column of W_1 so that its spectrum approximates the spectrum of the corresponding column of R_2. Call the result R_1. W_1 continues to denote the matrix with un-permuted column entries.
5) Apply the spectral mimicry algorithm to permute the entries of each column of W_1 so that its spectrum approximates the spectrum of the corresponding column of B_2. Call the result B_1. W_1 continues to denote the matrix with un-permuted column entries.
6) Define a matrix W of the same size as W_1 that has the entry 8g wherever W_1 has an entry less than 0, and the entry 80g wherever W_1 has an entry greater than 0.
7) Define a matrix R of the same size as R_1 that has the entry 8g wherever R_1 has an entry less than 0, and the entry 80g wherever R_1 has an entry greater than 0.
8) Define a matrix B of the same size as B_1 that has the entry 8g wherever B_1 has an entry less than 0, and the entry 80g wherever B_1 has an entry greater than 0.
9) The "W-numbers" (Methods) of each time series correspond to their column numbers in the matrices W, R and B, so that matched volume time series have the same W-numbers. Different W-numbers 1-5 were used for D1 and 6-10 were used for D2.

Appendix S1.2: LSD-LPA model parameter estimation

We fitted the LPA skeleton model with experimental data using the method of conditional least squares, following Dennis *et al.* (2001) and Cushing *et al.* (2003, pp. 113-118). The conditional sums of squares are:

$$Q_1(b, c_{el}, c_{ea}) = \sum_t \left(\sqrt{L_{t+1}} - \sqrt{bA_t \exp(-c_{el} L_t / V_t - c_{ea} A_t / V_t)} \right)^2$$

$$Q_2(\mu_l) = \sum_t \left(\sqrt{P_{t+1}} - \sqrt{(1-\mu_l) L_t} \right)^2$$

where V_t is the experimentally imposed habitat volume between time steps t and t+1, transformed to units of 20g, i.e., when 80g of flour were used, V_t = 4 and when 8g were used, V_t = 0.4. The sums are across time steps from all replicates. No formula was needed for the A equation of the LPA model because the parameters c_{pa} and μ_a were experimentally controlled. The conditional sums of squares were minimized separately, Q_2 using linear regression (without constant term), Q_1 using the Nelder-Mead simplex algorithm. The Nelder-Mead algorithm was run 50 times from randomly chosen starting points. Of the 50 results, the one with the lowest Q_1 was selected; the others corresponded to local minima of the objective function (Appendix S2).

Bootstrapped 95% confidence intervals for the parameters b, c_{el}, c_{ea}, and μ_l were obtained by the methods described in detail by Cushing *et al.* (2003, pp. 115-118). To obtain b, c_{el}, and c_{ea} for each set of bootstrapped parameters, the Nelder-Mead algorithm was run 50 times with randomly chosen initial parameters; results with the lowest Q_1 were taken as optimal. 2000 sets of bootstrapped parameters were obtained (Appendix S2).

The matrix Σ of the LSD-LPA model was estimated by covariance analysis of the vector residuals

$$D_t = (\sqrt{L_{t+1}} - \sqrt{bA_t \exp(-c_{el}L_t/V_t - c_{ea}A_t/V_t)}, \sqrt{P_{t+1}} - \sqrt{(1-\mu_l)L_t}).$$

Significance of the off-diagonal terms was assessed using the corresponding matrix of correlation coefficients.

The R^2 values for the fitted LPA model (one for the L stage and one for the P stage) were obtained by the formula 1-SSE/SST. SSE is the sum of the squared $D_{t,1}$ for L and $D_{t,2}$ for P. SST is $(\sqrt{L_{t+1}} - \text{mean}(\sqrt{L_{t+1}}))^2$ for the L stage and $(\sqrt{P_{t+1}} - \text{mean}(\sqrt{P_{t+1}}))^2$ for the P stage.

Appendix S1.3: The spectrum distance and shape fit tests

The spectrum distance and shape fit tests produce approximate *p*-values describing the fit in the frequency domain between a stochastic model and a data time series. We combined *p*-values of replicates produced by these methods to obtain one *p*-value per experimental treatment.

For the spectrum distance fit test, we sampled the distribution of L_2 distances between log spectra of model simulations and the mean model log spectrum by generating 10000 simulations of the same length as the data. The L_2 distance between two log spectra, f and g, was the square-root of the summed squared differences between f and g, the sum computed over normalized frequencies of the form 2s/T for s an integer from 0 to $\lfloor T/2 \rfloor$, where T is time series length. Distances between log spectra of replicate experimental time series and the mean model log spectrum were also computed, giving n values for n replicates. Whereas the spectrum distance fit test of Reuman *et al.* (2006) compared each data distance with the distribution of model distances to get a separate *p*-value for each replicate, we compared data and model distance distributions using a two-sample, one-sided Kolmogorov-Smirnov test. On samples of size a and b, the test is trustworthy only if a*b/(a+b) ≥ 4 (Matlab help files for "kstest2"), which held for treatments affected by noise, but not for the control treatments of this study. For those treatments, one *p*-value was produced for each of the three replicates and these were combined using the Fisher method. A similar procedure was used for the spectrum shape fit test.

A consistent spectral estimate of Brillinger (2001, *Time Series: Data Analysis and Theory*, p. 146) was used. This estimate, a type of smoothed periodogram, was chosen because, unlike the standard periodogram, it is asymptotically log-normally distributed over each frequency, making comparisons of sums of squared differences between log spectra reasonable, and making the mean log spectrum a reasonable measure of central tendency.

Appendix S1.4: Matching of model and data statistics

The validation methods of this study used many simulated time series of the same length as data. To compare the LSD-LPA model with data from a treatment in D1 (respectively, D2), the c_{pa} and μ_a values of D1 (respectively, D2) were used in the model. To compare the model to data from a treatment that was not exposed to environmental stochasticity, constant V_t = 44/20 time series (44 g of habitat medium) were used in the model. To compare the model to data from a treatment that was exposed to noise, V_t time series of the same color were used in the model. Spectral mimicry was used to generate colored V_t time series for the model just as it was used for the experiments, so that model V_t time series were distributed in the same way as experimental V_t time series.

To get *p*-values describing fit between a model and an experimental treatment using a time series statistic, the value of the statistic was computed for the b replicates of the treatment and for 10000 model-generated time series of the same length. If 10000*b/(10000+b) ≥ 4 (e.g., for the treatments affected by noise; see Appendix S1.3), a two-sample, two-sided Kolmogorov-Smirnov test was used to compare the distributions. Otherwise, a *p*-value was generated for each replicate by comparing its value of the statistic directly with those of the model-generated time series; replicate *p*-values were combined using the Fisher method.

Appendix S1.5: General methods

Most calculations were done in Matlab version 6.5.0.180913a (R13). ANOVAs were done in R version 2.5.1 using the nlme package. All logarithms were base 10.

Appendix S2: Supporting Results

Of the 50 Nelder-Mead minimizations of Q_1 (Appendix S1.2), 49 gave the same parameters to 6 decimal places. One Nelder-Mead run gave different parameters but had much higher Q_1 value. Best parameters rounded to 5 decimals are in Table S2.

Bootstrapped parameter estimates were approximately normally distributed (Fig. S2), and were not strongly correlated except b and c_{ea}, which had a correlation coefficient of 0.851. This correlation may indicate that the model is over-parameterized for the data of this study. However, Cushing *et al.* (2003, p. 118) concluded that all model degrees of freedom were needed to describe their data. We preferred to use a model that applies generally to the *T. castaneum* system, so we did not try to eliminate degrees of freedom from the model.

R^2 values for the LPA model with CLS parameters were 0.979 for the L stage and 0.996 for the P stage.

Table S1: Summary statistics for experimental data. Life-stage and total population means over time (A); variances over time (B); lag 4 autocorrelations minus lag 3 autocorrelations (C); log power at nf 0 and 1 (D). Columns 2-5 show means across treatments of each time series statistic computed for each replicate. Column 6 shows *p*-values for the effects of noise color within D1 and D2 separately. Column 7 shows *p*-values for the significance of interaction effects between noise color and dynamics treatment. ANOVAs exclude the no-noise treatments. Superscript * means residuals apparently violated the assumption of normality (1% level), but violations were not flagrant and were not considered problematic (Methods).

A

Dynamics treatment	No noise	Red noise	White noise	Blue noise	Noise color	Dynamics -noise int.
Mean total pop.						<0.0001
D1	788.0	728.0	901.1	1229.9	<0.0001	
D2	339.0	320.4	270.3	252.9	0.0134	
Mean L pop.						<0.0001
D1	237.3	228.2	293.8	383.0	<0.0001	
D2	146.8	134.5	111.4	102.3	0.0058	
Mean P pop.						<0.0001
D1	191.0	185.0	239.9	307.0	<0.0001	
D2	125.3	117.9	95.2	84.3	<0.0001	
Mean A pop.						<0.0001
D1	359.7	314.8	367.4	539.8	<0.0001	
D2	66.9	68.0	63.8	66.3	0.9194	

B

Dynamics treatment	No noise	Red noise	White noise	Blue noise	Noise color	Dynamics -noise int.
Variance of total pop.						0.3701
D1	30216.2	338437.7	268139.9	232665.3	0.0042	
D2	29992.8	107644.9	80438.0	59725.1	0.2838	
Variance of L pop.						<0.0001
D1	48852.0	111269.0	169131.3	189710.6	<0.0001	
D2	44100.4	77887.4	58800.7	47837.7	0.0144	
Variance of P pop.						<0.0001
D1	35561.7	78217.3	117074.4	130399.9	<0.0001	
D2	33960.2	60684.2	42277.3	33825.4	0.0015	
Variance of A pop.						0.8262
D1	11482.6	76080.2	68025.6	72087.2	0.5923	
D2	11587.7	21978.5	20576.7	19933.8	0.9648	

C

Dynamics treatment	No noise	Red noise	White noise	Blue noise	Noise color	Dynamics -noise int.
Autocorr. diff. tot. pop						0.0699*
D1	0.876	-0.045	-0.061	0.299	0.0008	
D2	-0.428	-0.243	-0.079	-0.028	0.0628	
Autocorr. diff. of L pop.						0.0003
D1	1.932	0.776	0.111	1.180	<0.0001	
D2	-1.292	-0.808	-0.291	-0.120	0.0022	
Autocorr. diff. of P pop.						0.0009
D1	1.895	0.709	0.107	1.176	<0.0001	
D2	-1.279	-0.828	-0.335	-0.088	0.0018	
Autocorr. diff. of A pop.						0.1782
D1	1.075	-0.018	-0.003	0.386	0.0047	
D2	-1.072	-0.634	-0.289	-0.110	0.0012	

D

Dynamics treatment	No noise	Red noise	White noise	Blue noise	Noise color	Dynamics -noise int.
Log power, nf 0, tot. pop.						0.9127
D1	4.04	5.34	4.99	4.87	0.0061	
D2	4.14	4.77	4.47	4.27	0.0058	
Log power, nf 0, L						0.3377
D1	2.52	4.35	4.01	3.50	0.0001	
D2	3.28	4.01	3.73	3.50	0.0245	
Log power, nf 0, P						0.9950
D1	3.00	4.18	3.87	3.66	0.0006	
D2	3.18	3.90	3.58	3.38	0.0005	
Log power, nf 0, A						0.3914*
D1	3.55	4.65	4.35	4.42	0.3112	
D2	3.16	3.55	3.39	3.07	0.0665	
Log power, nf 1, tot. pop.						0.0228
D1	4.05	4.19	4.28	4.58	0.0018	
D2	2.64	3.04	3.40	3.29	0.0049	
Log power, nf 1, L						0.0092
D1	4.63	4.71	4.77	5.10	0.0011	
D2	3.10	3.74	3.86	3.76	0.4273	
Log power, nf 1, P						0.0056
D1	4.47	4.53	4.60	4.93	0.0002	
D2	3.11	3.61	3.71	3.66	0.4831	
Log power, nf 1, A						0.0917
D1	3.70	3.74	3.77	4.16	0.0291	
D2	2.61	3.13	3.35	3.22	0.3934	

Table S2: Conditional least squares (CLS) best fitting parameters and 95% bootstrap confidence intervals of the LSD-LPA model for the data of this study, compared to parameters for the data of Dennis *et al.* (2001) and Cushing *et al.* (2003). The matrix of correlation coefficients corresponding to the covariance matrix $\Sigma = (\sigma_{ij})$ had off-diagonal elements σ_{12} not significantly different from 0 for both datasets ($p = 0.191$ for the present data), so diagonal Σ was used for all model validations and predictions, i.e., E_{1t} and E_{2t} were uncorrelated in time. While the point estimates look roughly similar, the confidence intervals from one experiment do not include the point estimates from the other experiment for most of the parameters. The experiments differed in that this study's experiment imposed environmental noise in the form of habitat volume fluctuations while the other experiment had constant habitat volumes lower than the mean habitat volume of this study's experiment.

	Using the data of this study		Using Dennis *et al.* data	
Parameter	CLS parameters	95% conf. ints.	CLS parameters	95% conf. ints.
b	9.82349	(9.58810, 10.04252)	10.45	(10.04, 10.77)
c_{el}	0.01657	(0.01606, 0.01689)	0.01731	(0.01611, 0.01759)
c_{ea}	0.01300	(0.01277, 0.01322)	0.01310	(0.01285, 0.01340)
μ_l	0.15723	(0.15274, 0.16177)	0.2000	(0.1931, 0.2068)
σ_{11}	2.46969	--	2.332	--
σ_{12}	-0.03568	NS	0.007097	NS
σ_{22}	0.43289	--	0.2374	--

Figure S1: Time series for one representative replicate per experimental treatment: no imposed environmental noise (A); red noise (B); white noise (C); and blue noise (D). Panels on the left are dynamics regime D1, those on the right are dynamics regime D2. Time series on the left (respectively, right) in B-D have the same W numbers. Volumes, V, are in grams. Oscillations of period 4 fortnights can be detected visually in the right panels of D.

A

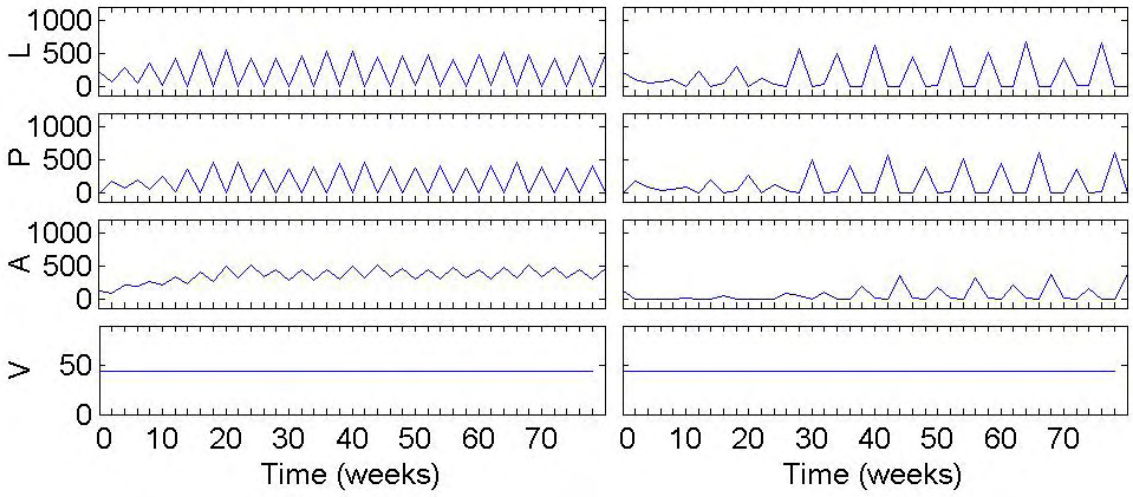

B

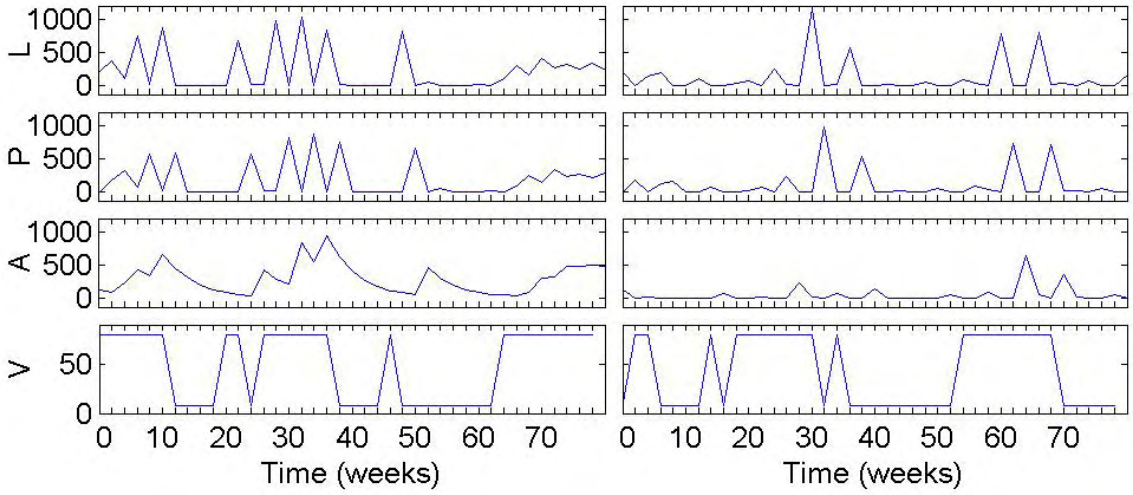

C

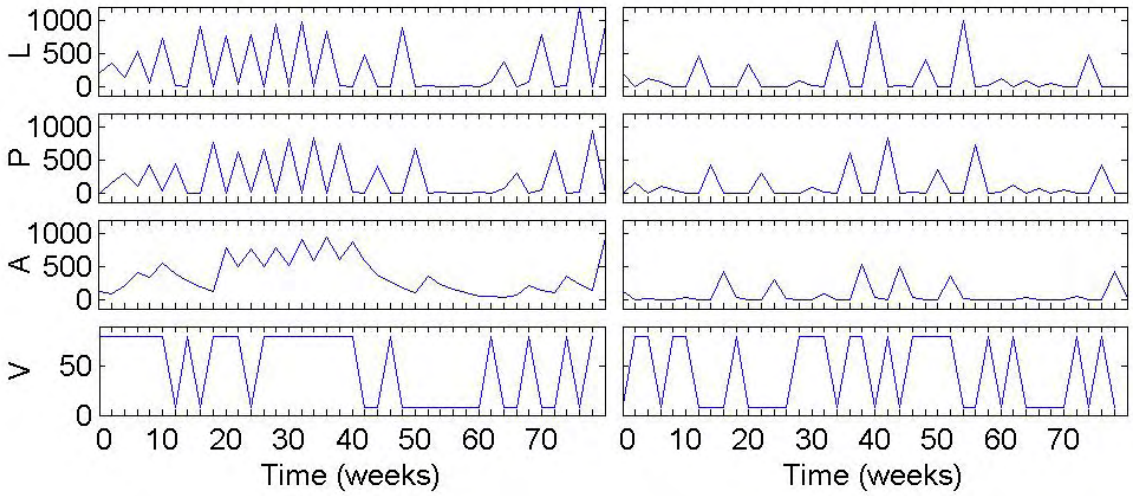
L
P
A
V
1000
500
0
50
0 10 20 30 40 50 60 70
Time (weeks)

D

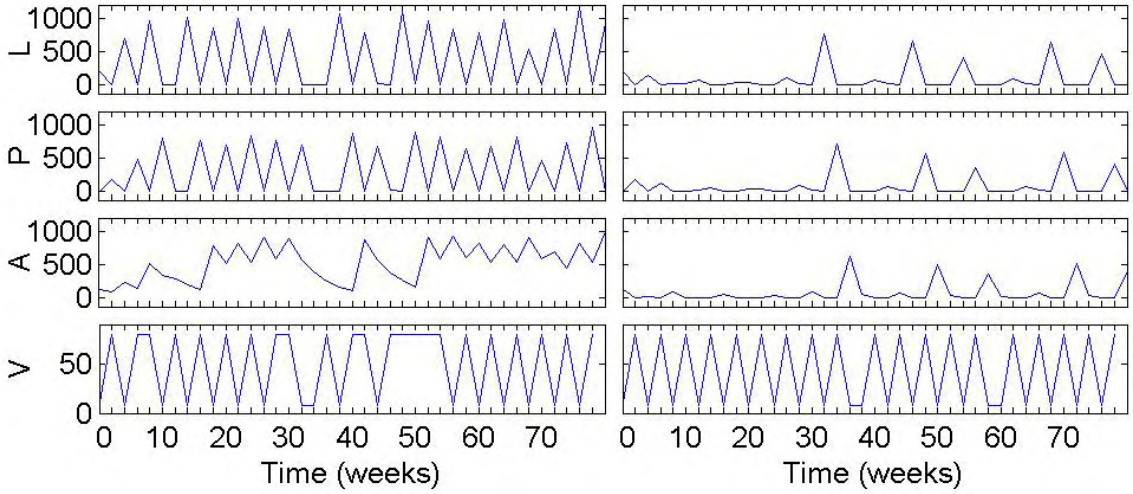
L
P
A
V
1000
500
0
50
0 10 20 30 40 50 60 70
Time (weeks)

Figure S2: (A) Quantile-quantile plots for the standardized (std.) bootstrapped parameter estimates of b, c_{el}, c_{ea}, μ_l. (B) A scatter plot matrix of the 2000 standardized bootstrapped estimates of b, c_{el}, c_{ea}, μ_l. Numbers on the y-axis do not apply to the histograms but do apply to the scatter plots. Correlation coefficients were <0.17 except that between b and c_{ea}, which was 0.851.

A

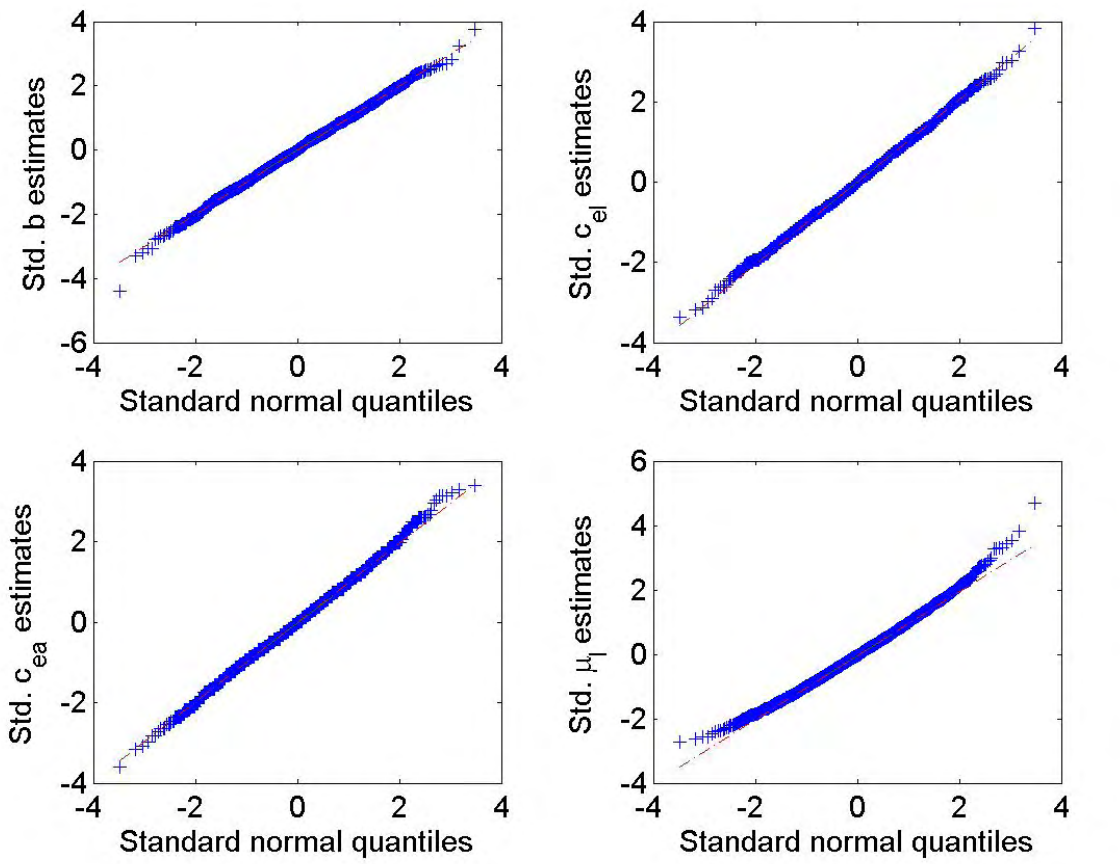

182 **B**

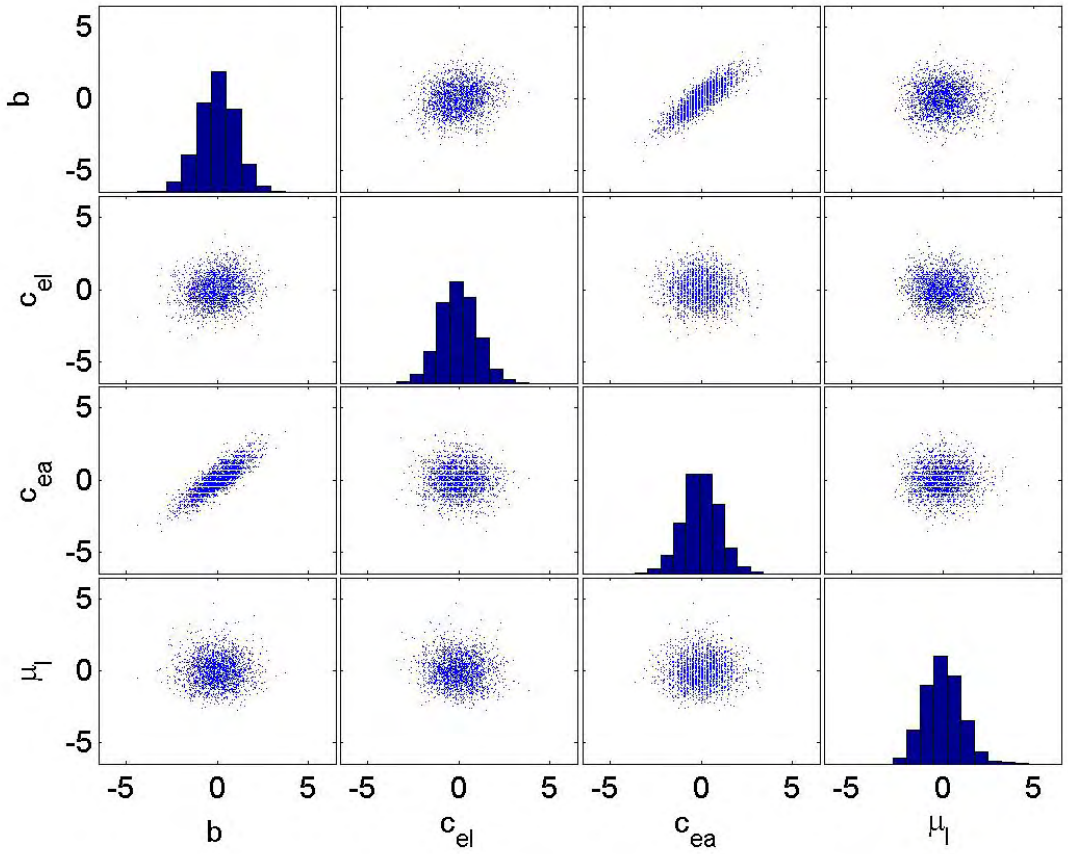

183

Figure S3: Frequency-domain validation (plots on the main diagonal of each array) and cross comparison (plots off the main diagonal of each array) of the LSD-LPA model with data: (A) L-stage; (B) P-stage; (C) A-stage. Red lines are log spectra of life-stage time series and are the same in all panels within a column. Columns correspond to experimental treatments. Indicated in red above the columns, the first four are for D1 and the last four are for D2. The color of environmental noise imposed is listed in red below each column. Black lines are 2.5th, 25th, 50th, 75th, and 97.5th percentiles over each frequency of log spectra of 10000 model generated life-stage time series; they are the same in all panels in a row. Indicated in black to the right of the rows, D1 was used in the model for the top 4 rows and D2 for the bottom 4 rows. The color of the V_t time series used in the model is listed in black to the left of each row. Panels for which model and experimental treatments were the same (on the main diagonal) are yellow to ease viewing. For (A), these are the same as Fig. 3A. Panels show spectrum distance (upper left) and spectrum shape (upper right) fit test *p*-value results. *P*-values describe the fit of all life stages. Table 3 parameters were used in the model.

200 **A**

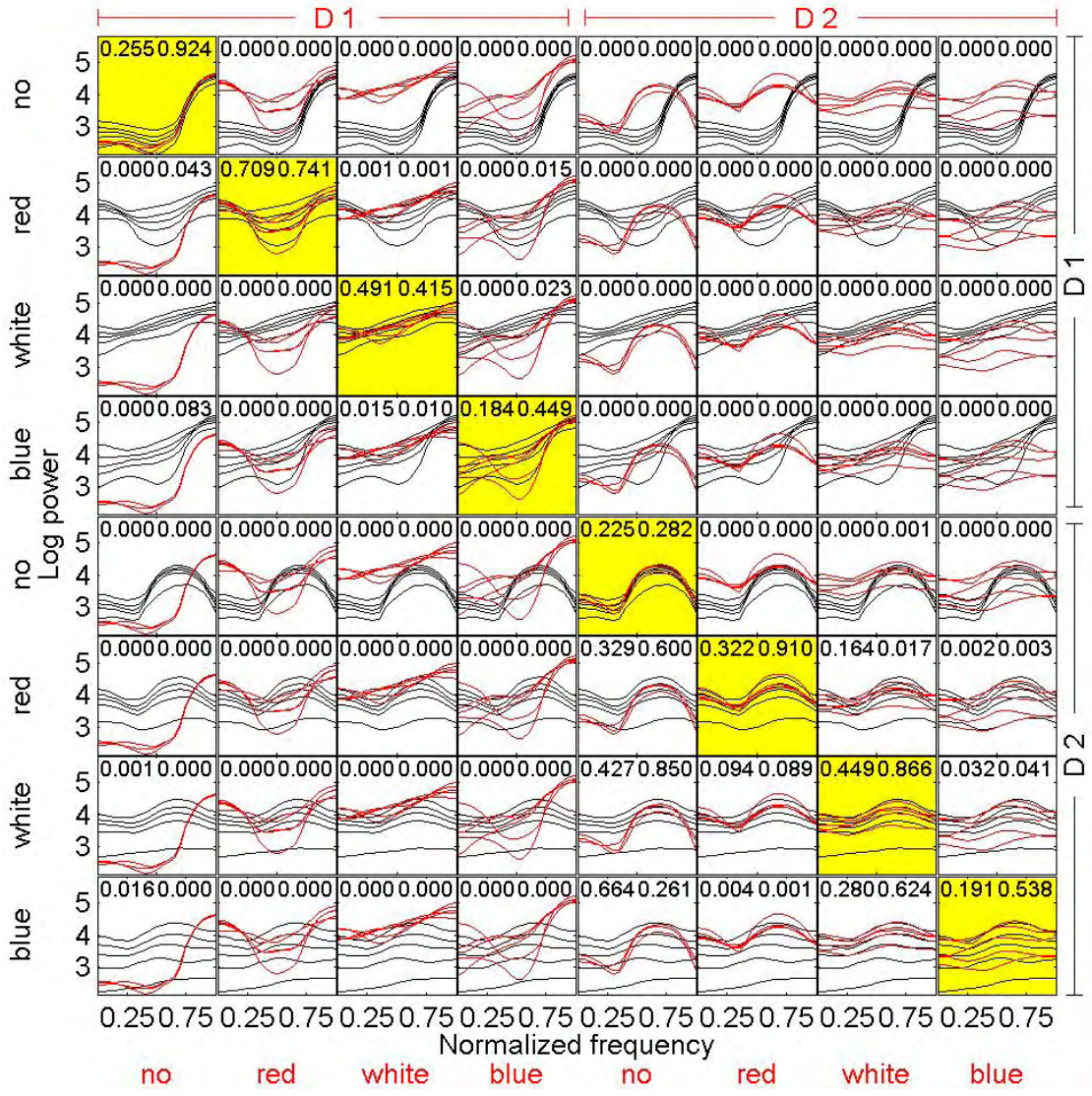
D 1
D 2
no
red
white
blue
Log power
D 1
D 2
0.25 0.75
Normalized frequency
no
red
white
blue

201

B

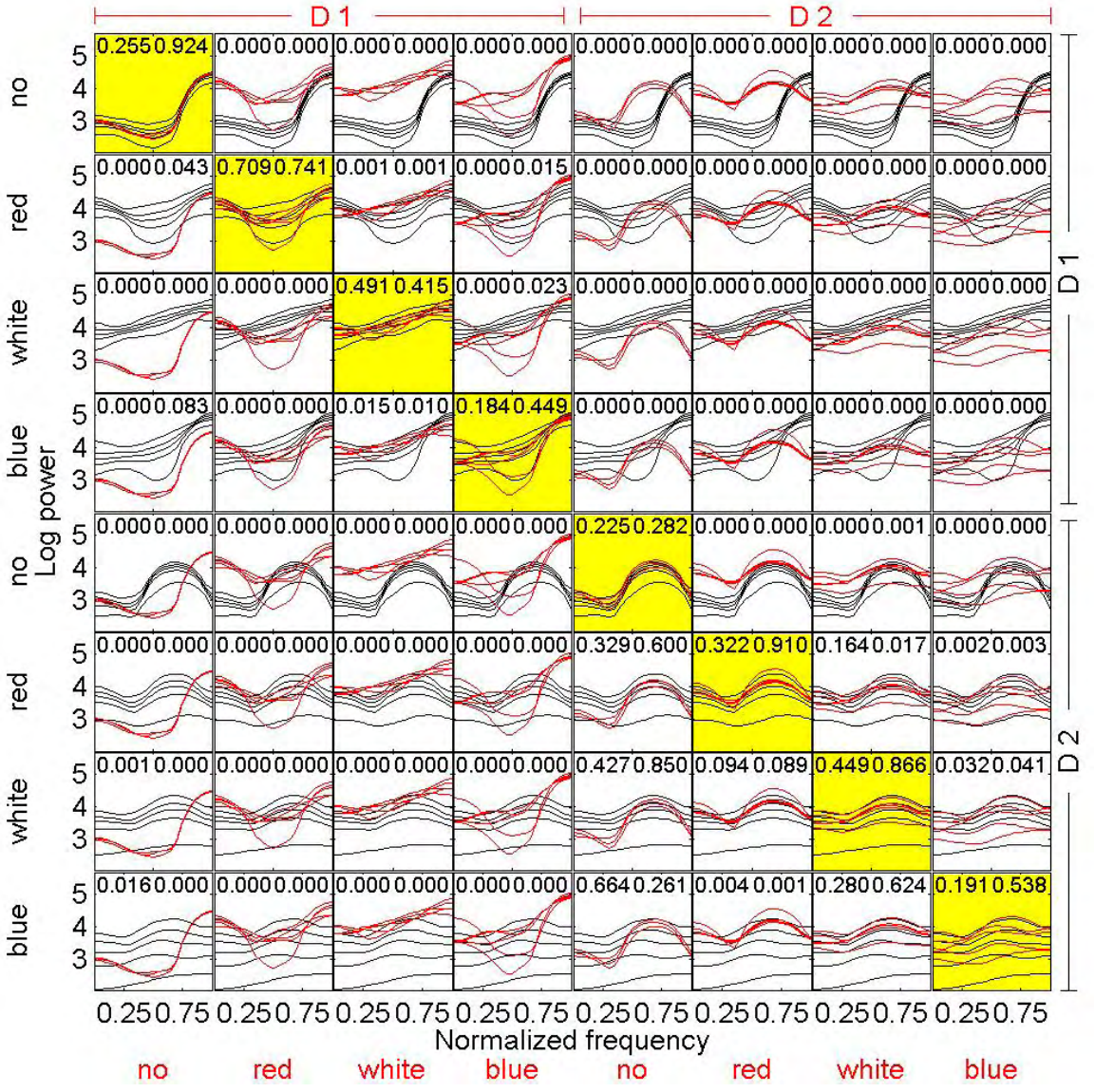
D 1
D 2
no
red
white
blue
Log power
5
4
3
0.255 0.924
0.000 0.000
0.000 0.000
0.000 0.000
0.000 0.000
0.000 0.000
0.000 0.000
0.000 0.000
0.000 0.043
0.709 0.741
0.001 0.001
0.000 0.015
0.000 0.000
0.000 0.000
0.000 0.000
0.000 0.000
0.000 0.000
0.000 0.000
0.491 0.415
0.000 0.023
0.000 0.000
0.000 0.000
0.000 0.000
0.000 0.000
0.000 0.083
0.000 0.000
0.015 0.010
0.184 0.449
0.000 0.000
0.000 0.000
0.000 0.000
0.000 0.000
0.000 0.000
0.000 0.000
0.000 0.000
0.000 0.000
0.225 0.282
0.000 0.000
0.000 0.001
0.000 0.000
0.000 0.000
0.000 0.000
0.000 0.000
0.000 0.000
0.329 0.600
0.322 0.910
0.164 0.017
0.002 0.003
0.001 0.000
0.000 0.000
0.000 0.000
0.000 0.000
0.427 0.850
0.094 0.089
0.449 0.866
0.032 0.041
0.016 0.000
0.000 0.000
0.000 0.000
0.000 0.000
0.664 0.261
0.004 0.001
0.280 0.624
0.191 0.538
0.25 0.75
Normalized frequency
no
red
white
blue

C

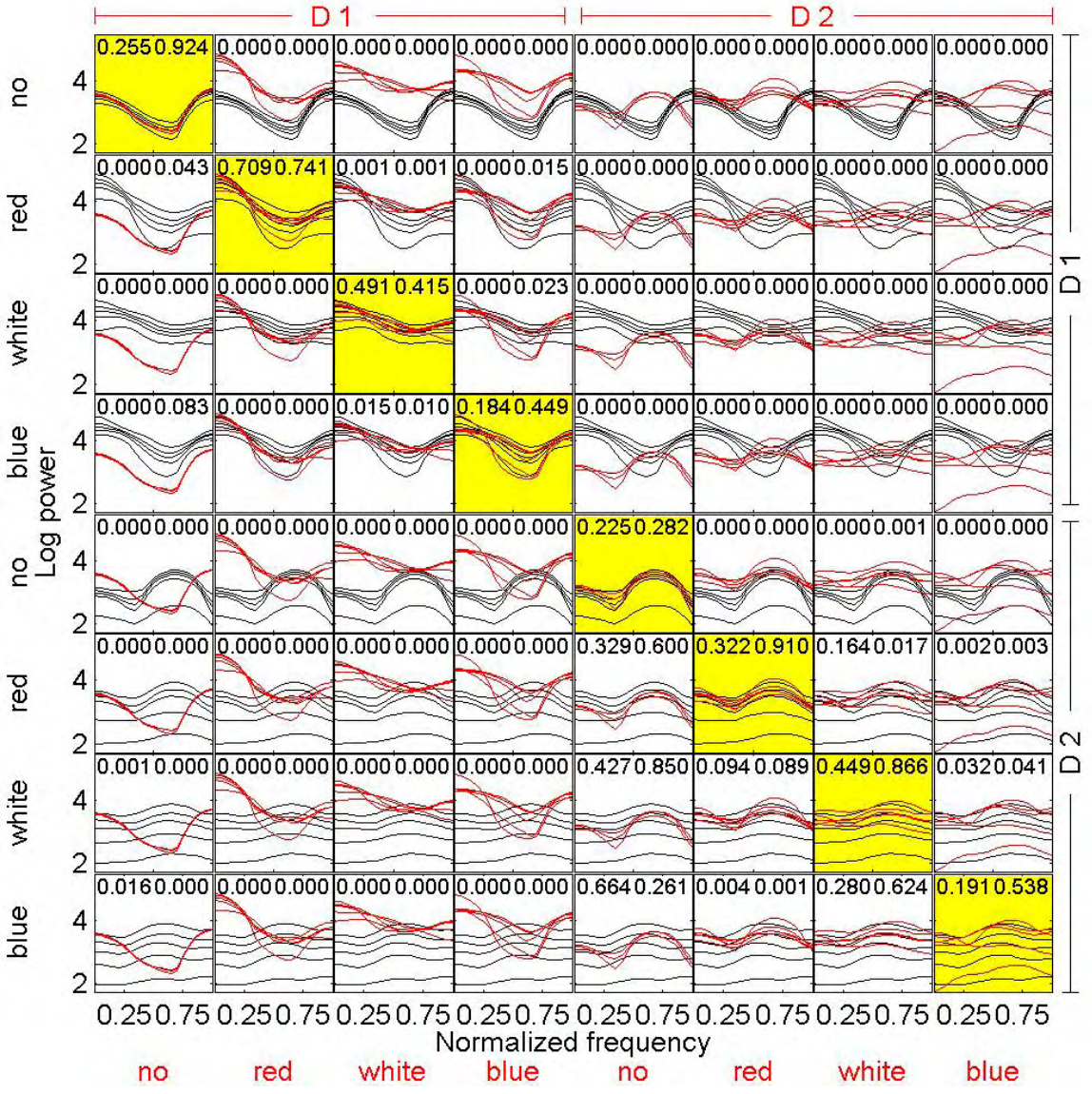
D 1
D 2
no
red
white
blue
Log power
0.255 0.924
0.000 0.000
0.000 0.000
0.000 0.000
0.000 0.000
0.000 0.000
0.000 0.000
0.000 0.000
0.000 0.043
0.709 0.741
0.001 0.001
0.000 0.015
0.000 0.000
0.000 0.000
0.000 0.000
0.000 0.000
0.000 0.000
0.000 0.000
0.491 0.415
0.000 0.023
0.000 0.000
0.000 0.000
0.000 0.000
0.000 0.000
0.000 0.083
0.000 0.000
0.015 0.010
0.184 0.449
0.000 0.000
0.000 0.000
0.000 0.000
0.000 0.000
0.000 0.000
0.000 0.000
0.000 0.000
0.000 0.000
0.225 0.282
0.000 0.000
0.000 0.001
0.000 0.000
0.000 0.000
0.000 0.000
0.000 0.000
0.000 0.000
0.329 0.600
0.322 0.910
0.164 0.017
0.002 0.003
0.001 0.000
0.000 0.000
0.000 0.000
0.000 0.000
0.427 0.850
0.094 0.089
0.449 0.866
0.032 0.041
0.016 0.000
0.000 0.000
0.000 0.000
0.000 0.000
0.664 0.261
0.004 0.001
0.280 0.624
0.191 0.538
2
4
0.25 0.75
Normalized frequency

Figure S4: Validation and cross comparison of the LSD-LPA model with data using the mean total (A), mean L-stage (B), mean P-stage (C), and mean A-stage (D) population statistics; the variances of the total population (E), the L-stage (F), the P-stage (G), and the A-stage (H); $R(4) - R(3)$ for the total population (I), the L-stage (J), the P-stage (K), and the A-stage (L). Red vertical lines are statistics for experimental replicates, and are the same in all panels in a column. Each column corresponds to one experimental treatment. As indicated in red above the columns, the first four correspond to D1 and the last four correspond to D2. The color of environmental stochasticity imposed on the treatment is listed in red below each column. Histograms show distributions of the statistics for 10000 model simulations, and are the same for all panels in a row. As indicated in black to the right of the rows, D1 was used in the model for the top 4 rows and D2 was used for the bottom 4 rows. The color of the V_t time series used in the model is listed in black to the left of each row. Panels for which the model and experimental treatments were the same are highlighted yellow. For (A), these diagonal panels are the same as Fig. 3B. Each panel shows a *p*-value for a test of the null hypothesis that model and data distributions are the same.

A

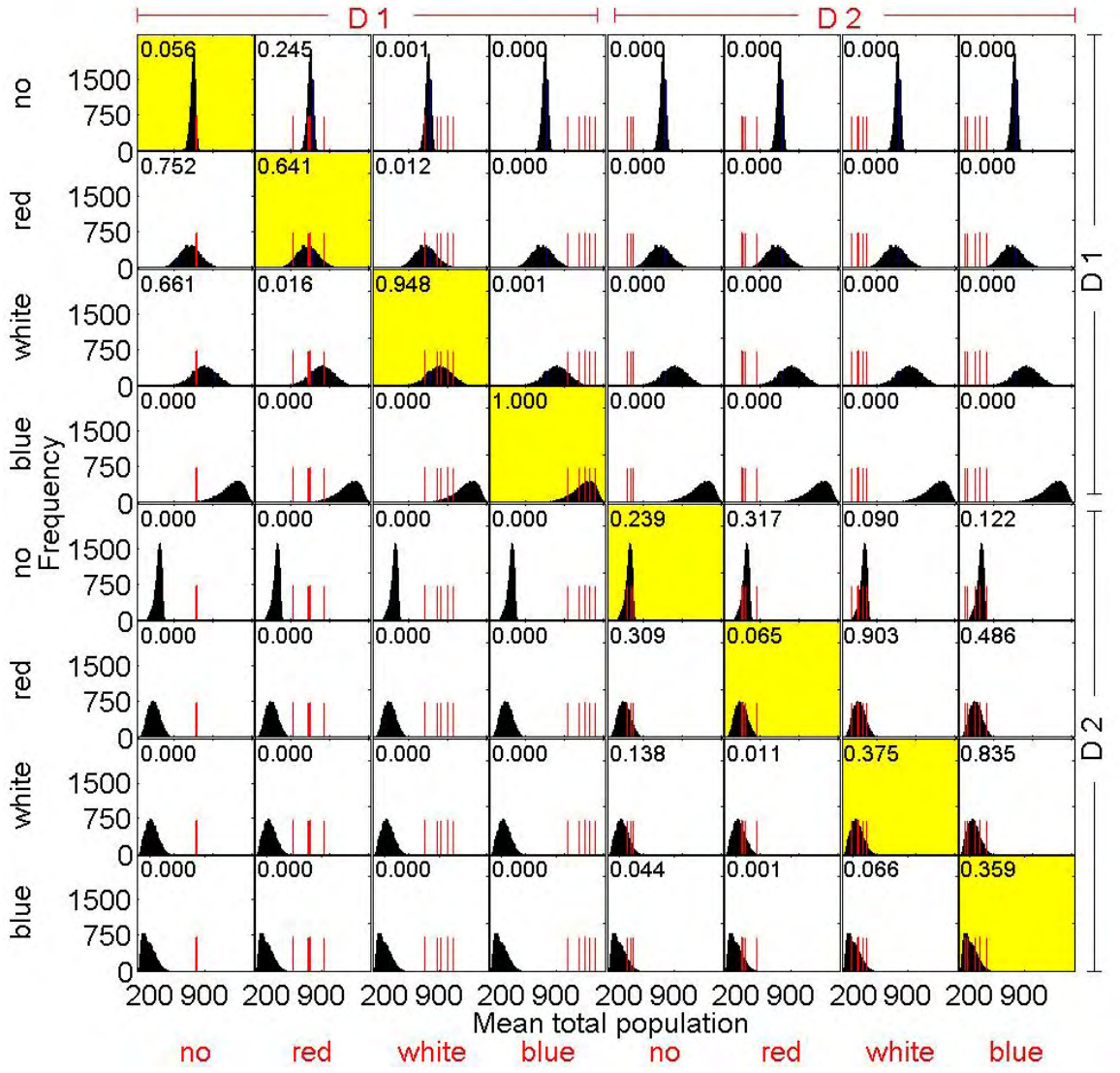
D 1
D 2
no
red
white
blue
Frequency
1500
750
0
0.056 0.245 0.001 0.000 0.000 0.000 0.000 0.000
0.752 0.641 0.012 0.000 0.000 0.000 0.000 0.000
0.661 0.016 0.948 0.001 0.000 0.000 0.000 0.000
0.000 0.000 0.000 1.000 0.000 0.000 0.000 0.000
0.000 0.000 0.000 0.000 0.239 0.317 0.090 0.122
0.000 0.000 0.000 0.000 0.309 0.065 0.903 0.486
0.000 0.000 0.000 0.000 0.138 0.011 0.375 0.835
0.000 0.000 0.000 0.000 0.044 0.001 0.066 0.359
200 900
Mean total population
no red white blue no red white blue

B

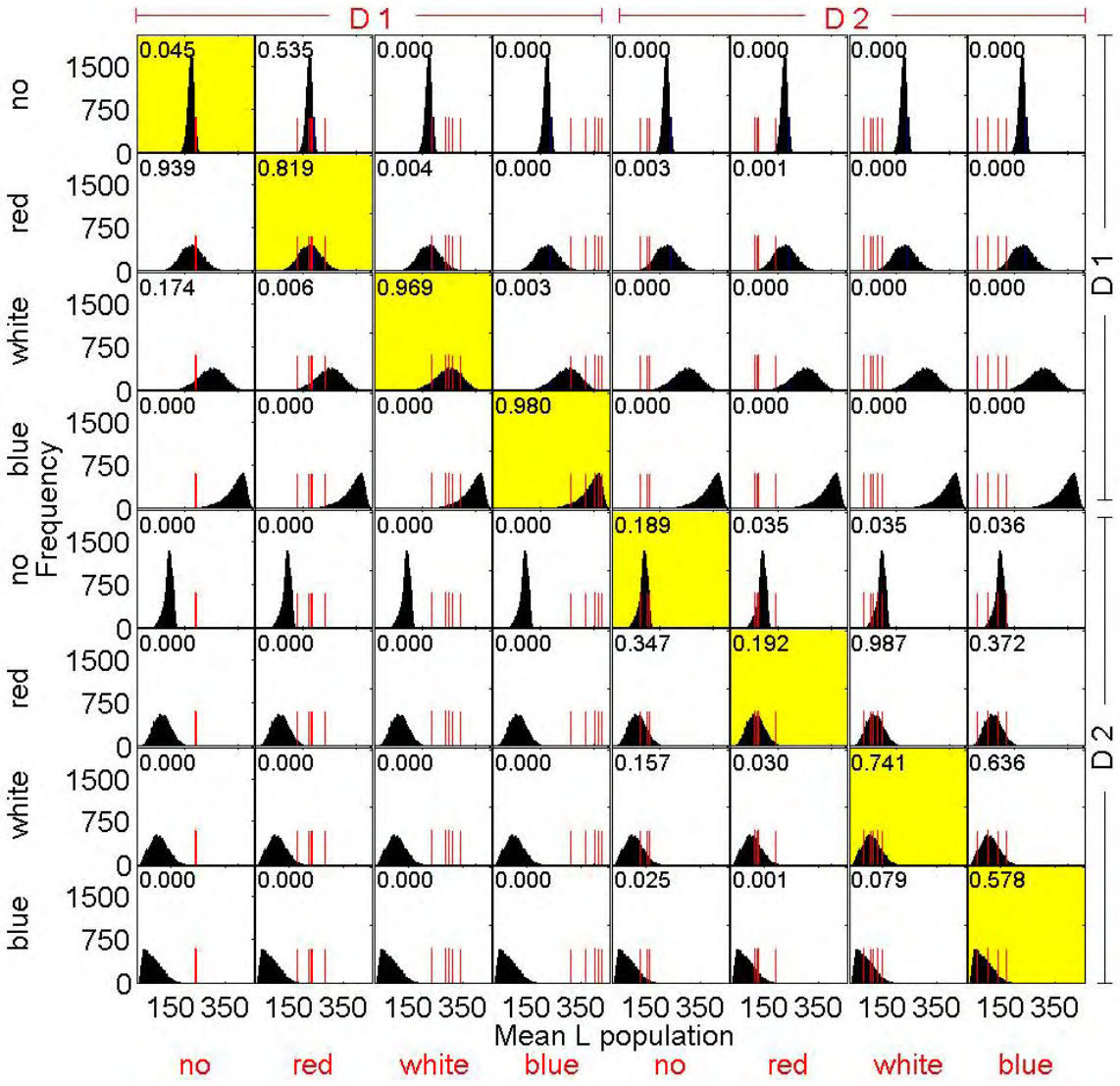
D 1
D 2
no
red
white
blue
Frequency
0 750 1500
0.045 0.535 0.000 0.000 0.000 0.000 0.000 0.000
0.939 0.819 0.004 0.000 0.003 0.001 0.000 0.000
0.174 0.006 0.969 0.003 0.000 0.000 0.000 0.000
0.000 0.000 0.000 0.980 0.000 0.000 0.000 0.000
0.000 0.000 0.000 0.000 0.189 0.035 0.035 0.036
0.000 0.000 0.000 0.000 0.347 0.192 0.987 0.372
0.000 0.000 0.000 0.000 0.157 0.030 0.741 0.636
0.000 0.000 0.000 0.000 0.025 0.001 0.079 0.578
150 350
Mean L population
no red white blue no red white blue

228 **C**

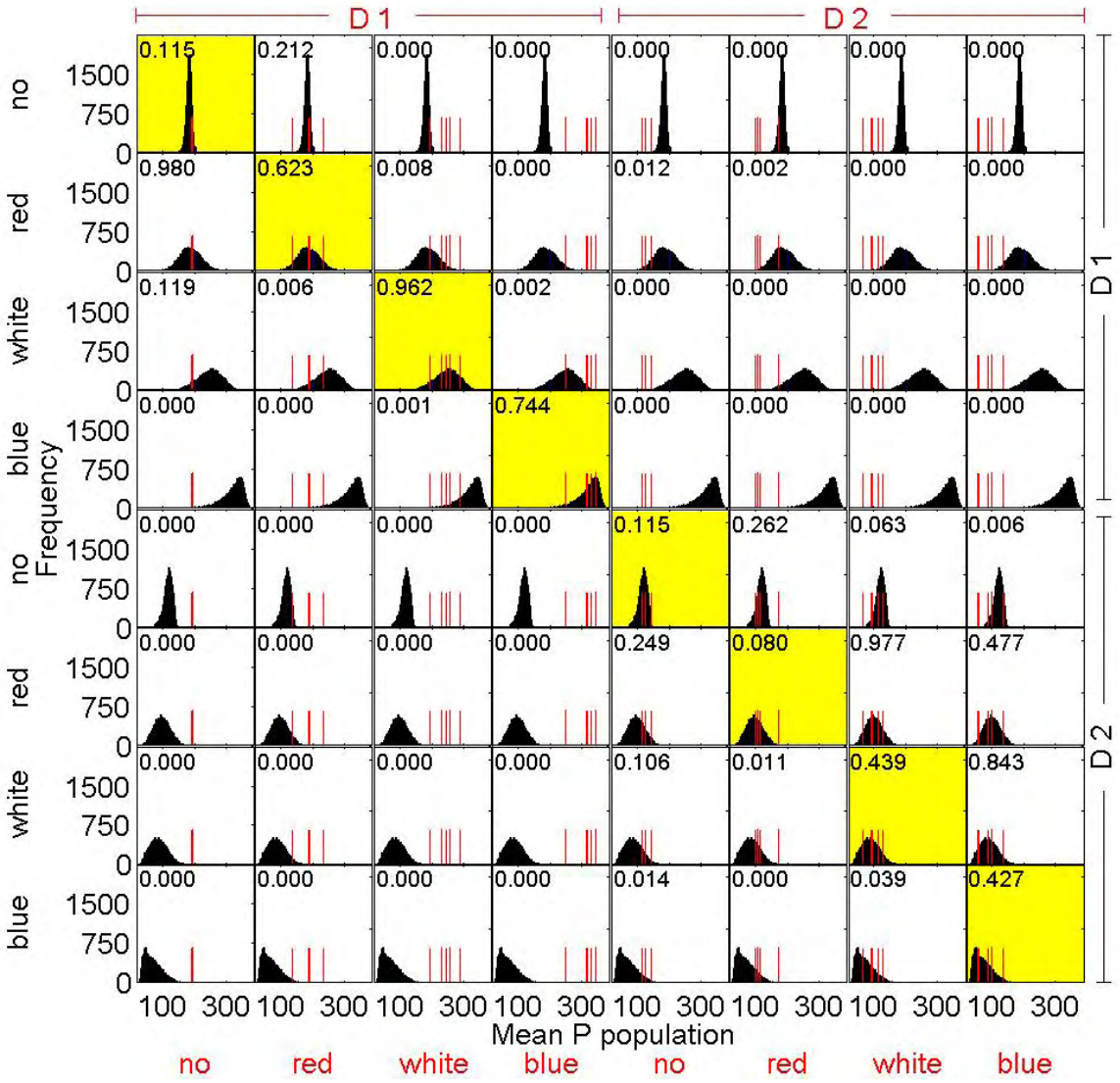
D 1
D 2
no
red
white
blue
Frequency
1500
750
0
0.115 0.212 0.000 0.000 0.000 0.000 0.000 0.000
0.980 0.623 0.008 0.000 0.012 0.002 0.000 0.000
0.119 0.006 0.962 0.002 0.000 0.000 0.000 0.000
0.000 0.000 0.001 0.744 0.000 0.000 0.000 0.000
0.000 0.000 0.000 0.000 0.115 0.262 0.063 0.006
0.000 0.000 0.000 0.000 0.249 0.080 0.977 0.477
0.000 0.000 0.000 0.000 0.106 0.011 0.439 0.843
0.000 0.000 0.000 0.000 0.014 0.000 0.039 0.427
100 300
Mean P population
no red white blue no red white blue

229

D

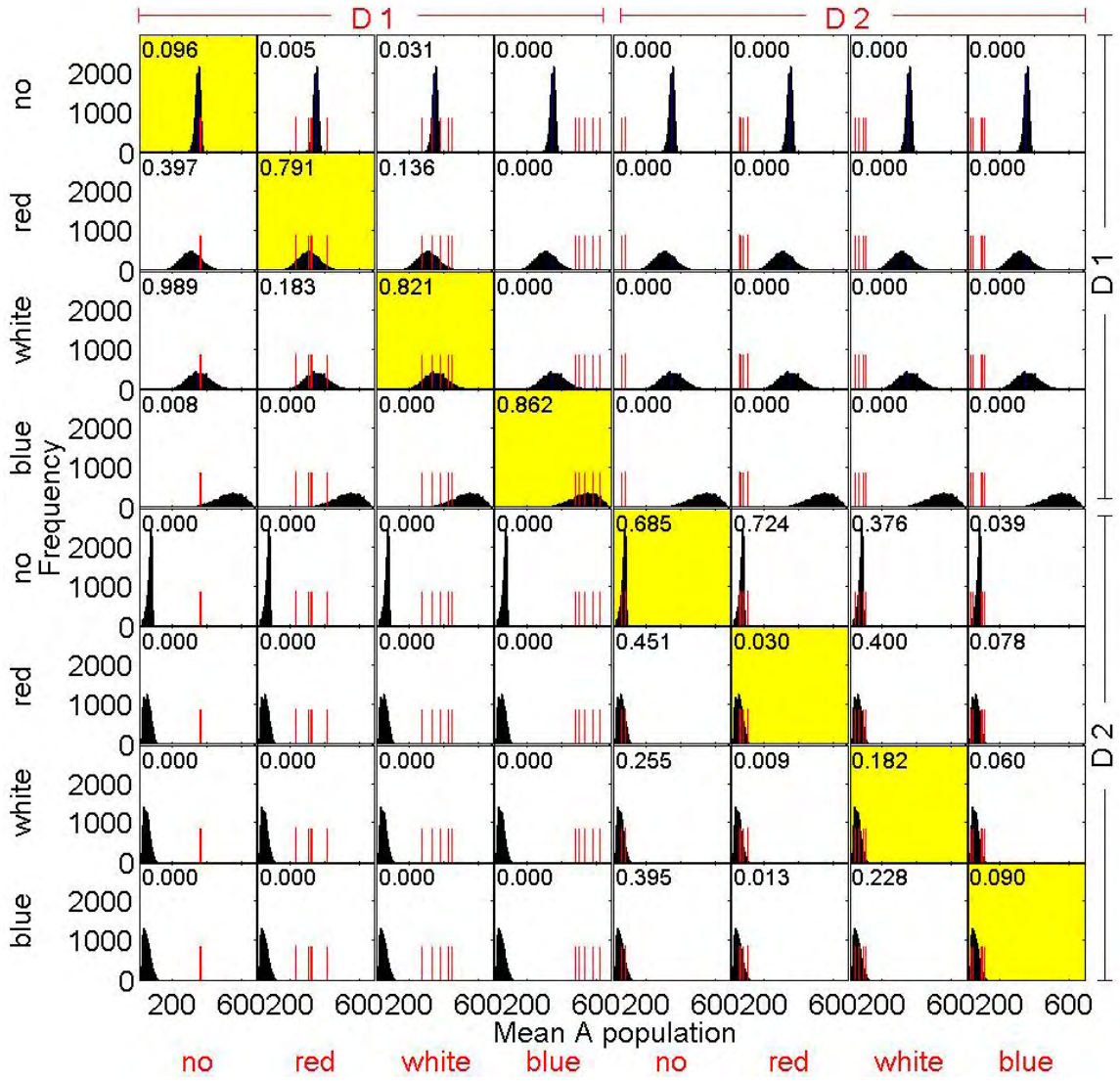
D 1
D 2
no
red
white
blue
Frequency
2000
1000
0
0.096 0.005 0.031 0.000 0.000 0.000 0.000 0.000
0.397 0.791 0.136 0.000 0.000 0.000 0.000 0.000
0.989 0.183 0.821 0.000 0.000 0.000 0.000 0.000
0.008 0.000 0.000 0.862 0.000 0.000 0.000 0.000
0.000 0.000 0.000 0.000 0.685 0.724 0.376 0.039
0.000 0.000 0.000 0.000 0.451 0.030 0.400 0.078
0.000 0.000 0.000 0.000 0.255 0.009 0.182 0.060
0.000 0.000 0.000 0.000 0.395 0.013 0.228 0.090
200 600200 600200 600200 600200 600200 600200 600200 600
Mean A population
no red white blue no red white blue

232 **E**

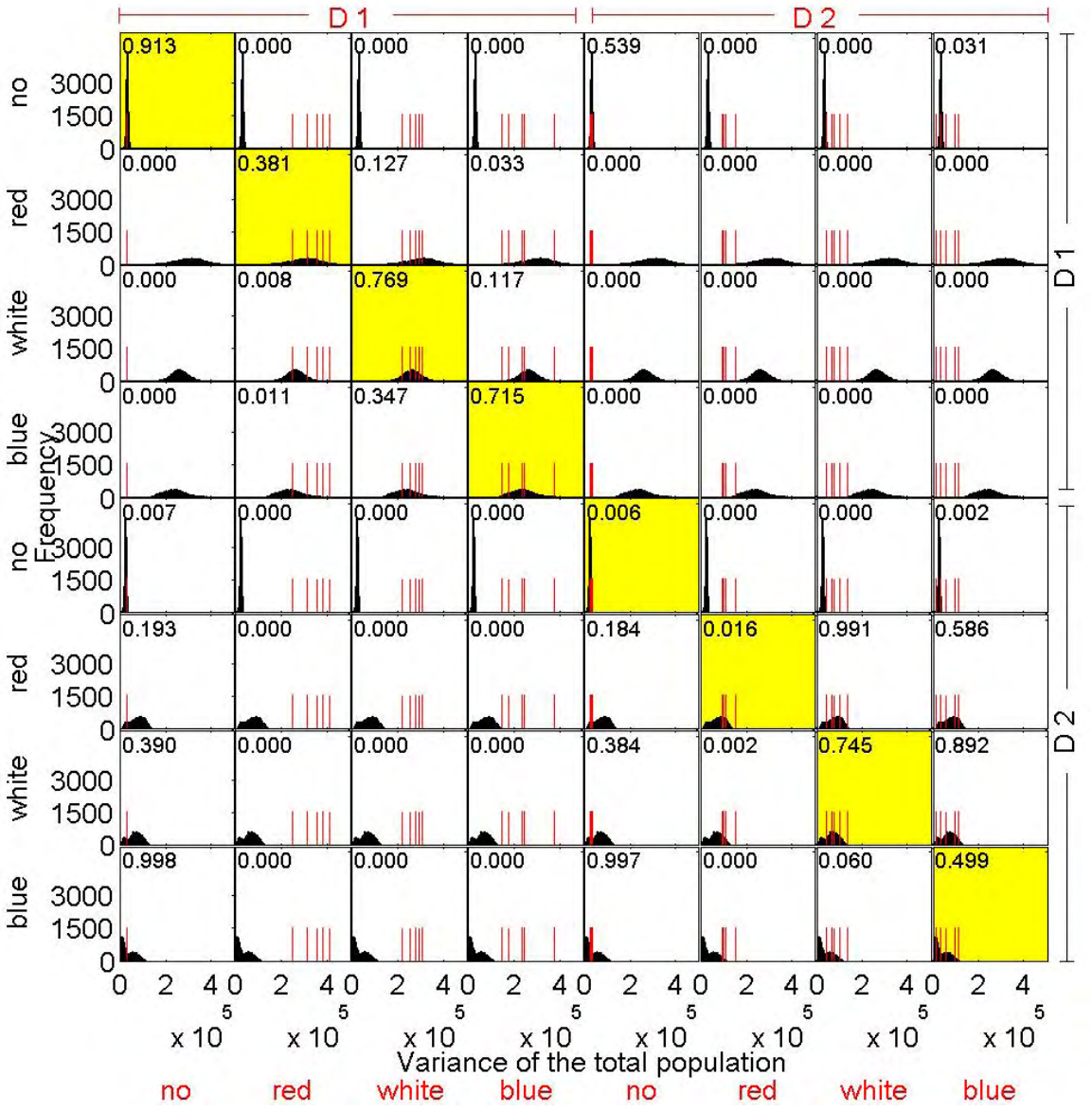
D 1
D 2
0.913 0.000 0.000 0.000 0.539 0.000 0.000 0.031
0.000 0.381 0.127 0.033 0.000 0.000 0.000 0.000
0.000 0.008 0.769 0.117 0.000 0.000 0.000 0.000
0.000 0.011 0.347 0.715 0.000 0.000 0.000 0.000
0.007 0.000 0.000 0.000 0.006 0.000 0.000 0.002
0.193 0.000 0.000 0.000 0.184 0.016 0.991 0.586
0.390 0.000 0.000 0.000 0.384 0.002 0.745 0.892
0.998 0.000 0.000 0.000 0.997 0.000 0.060 0.499
no
red
white
blue
3000
1500
0
Frequency
x 10^5
Variance of the total population
no red white blue no red white blue

233

F

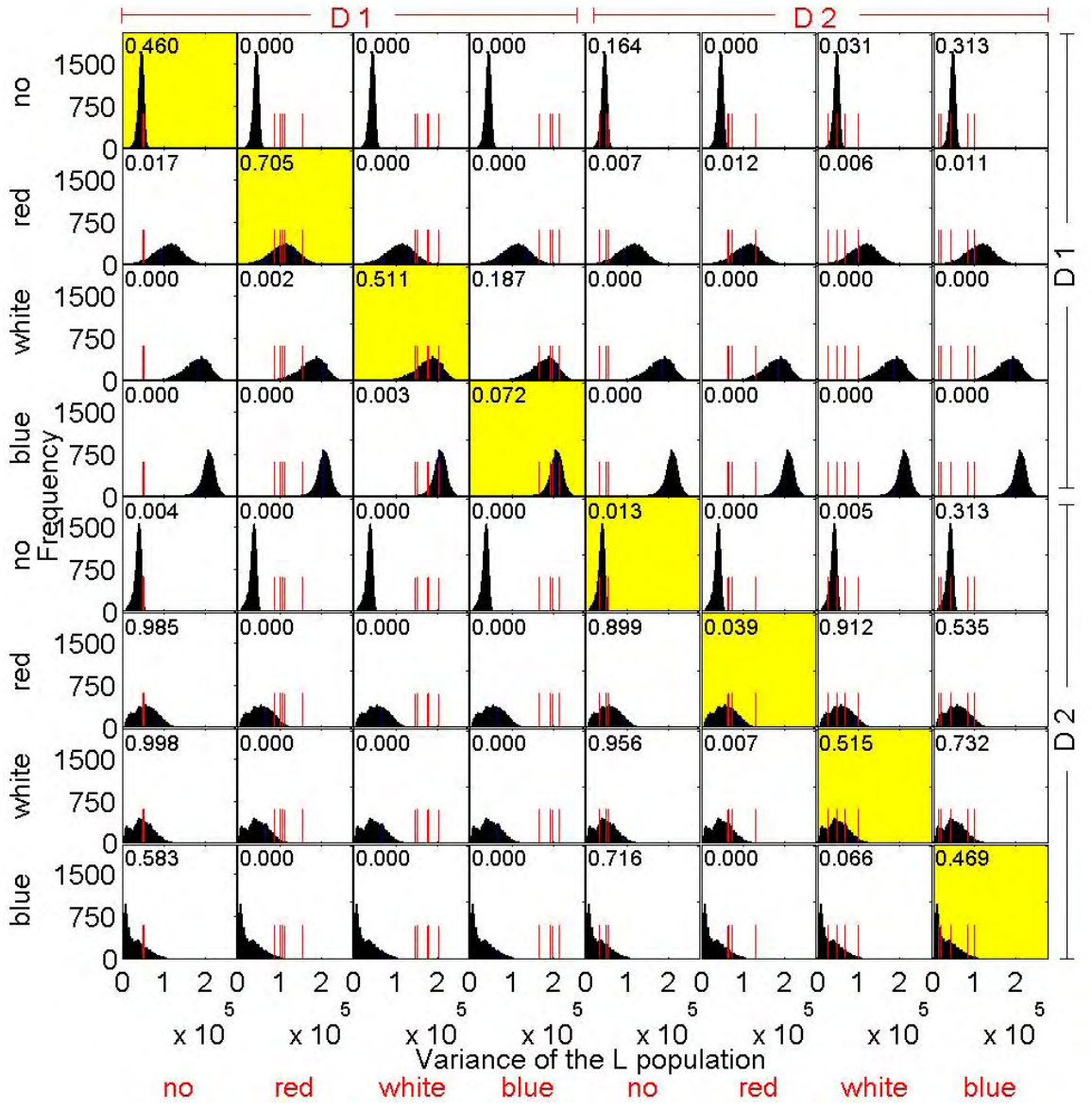
D 1
D 2
0.460 0.000 0.000 0.000 0.164 0.000 0.031 0.313
0.017 0.705 0.000 0.000 0.007 0.012 0.006 0.011
0.000 0.002 0.511 0.187 0.000 0.000 0.000 0.000
0.000 0.000 0.003 0.072 0.000 0.000 0.000 0.000
0.004 0.000 0.000 0.000 0.013 0.000 0.005 0.313
0.985 0.000 0.000 0.000 0.899 0.039 0.912 0.535
0.998 0.000 0.000 0.000 0.956 0.007 0.515 0.732
0.583 0.000 0.000 0.000 0.716 0.000 0.066 0.469
no
red
white
blue
Frequency
1500
750
0
0 1 2
x 10^5
Variance of the L population
no red white blue no red white blue

G

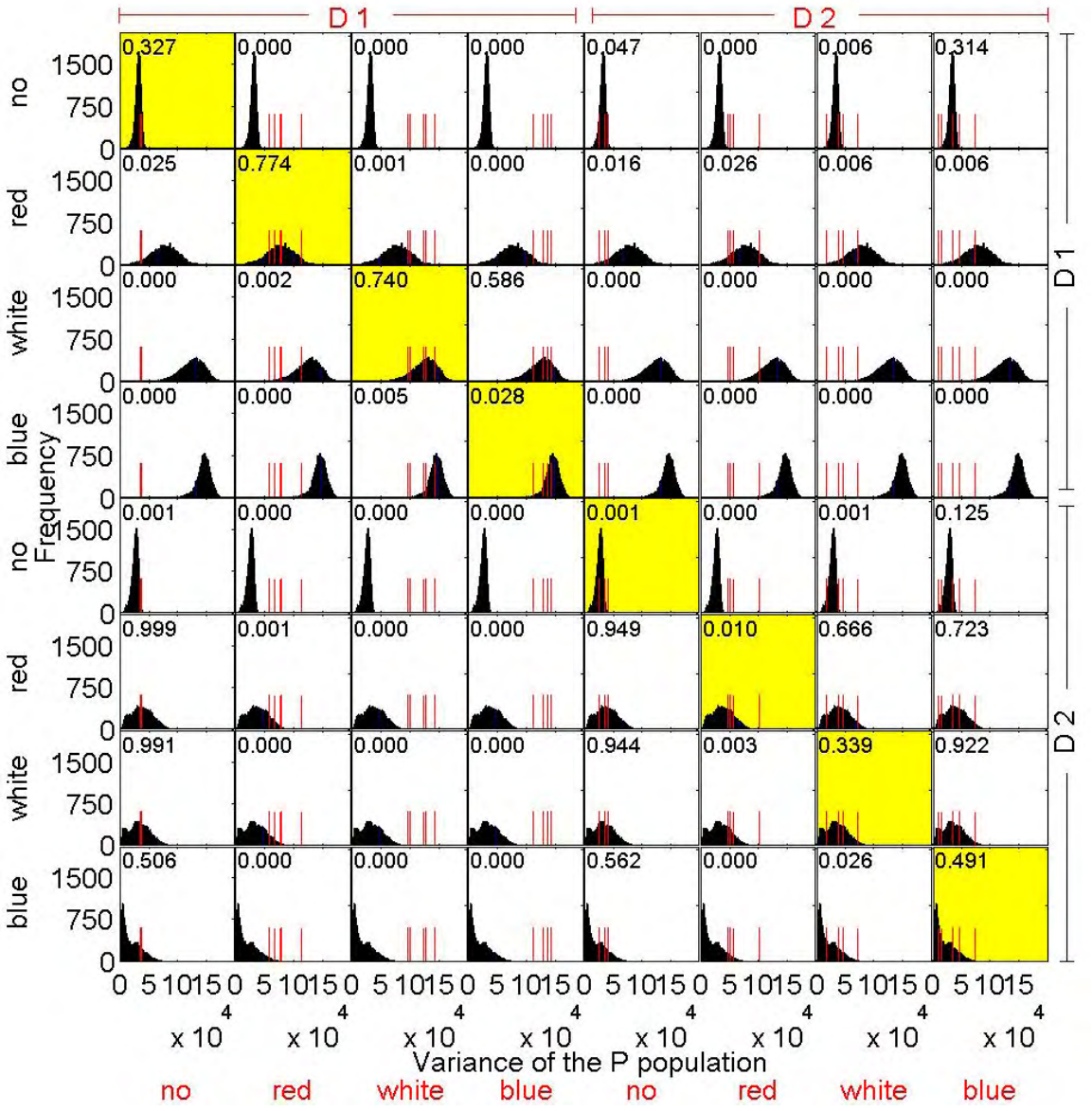
D 1
D 2
no
red
white
blue
Frequency
0.327 0.000 0.000 0.000 0.047 0.000 0.006 0.314
0.025 0.774 0.001 0.000 0.016 0.026 0.006 0.006
0.000 0.002 0.740 0.586 0.000 0.000 0.000 0.000
0.000 0.000 0.005 0.028 0.000 0.000 0.000 0.000
0.001 0.000 0.000 0.000 0.001 0.000 0.001 0.125
0.999 0.001 0.000 0.000 0.949 0.010 0.666 0.723
0.991 0.000 0.000 0.000 0.944 0.003 0.339 0.922
0.506 0.000 0.000 0.000 0.562 0.000 0.026 0.491
0 5 10 15
x 10^4
Variance of the P population

H

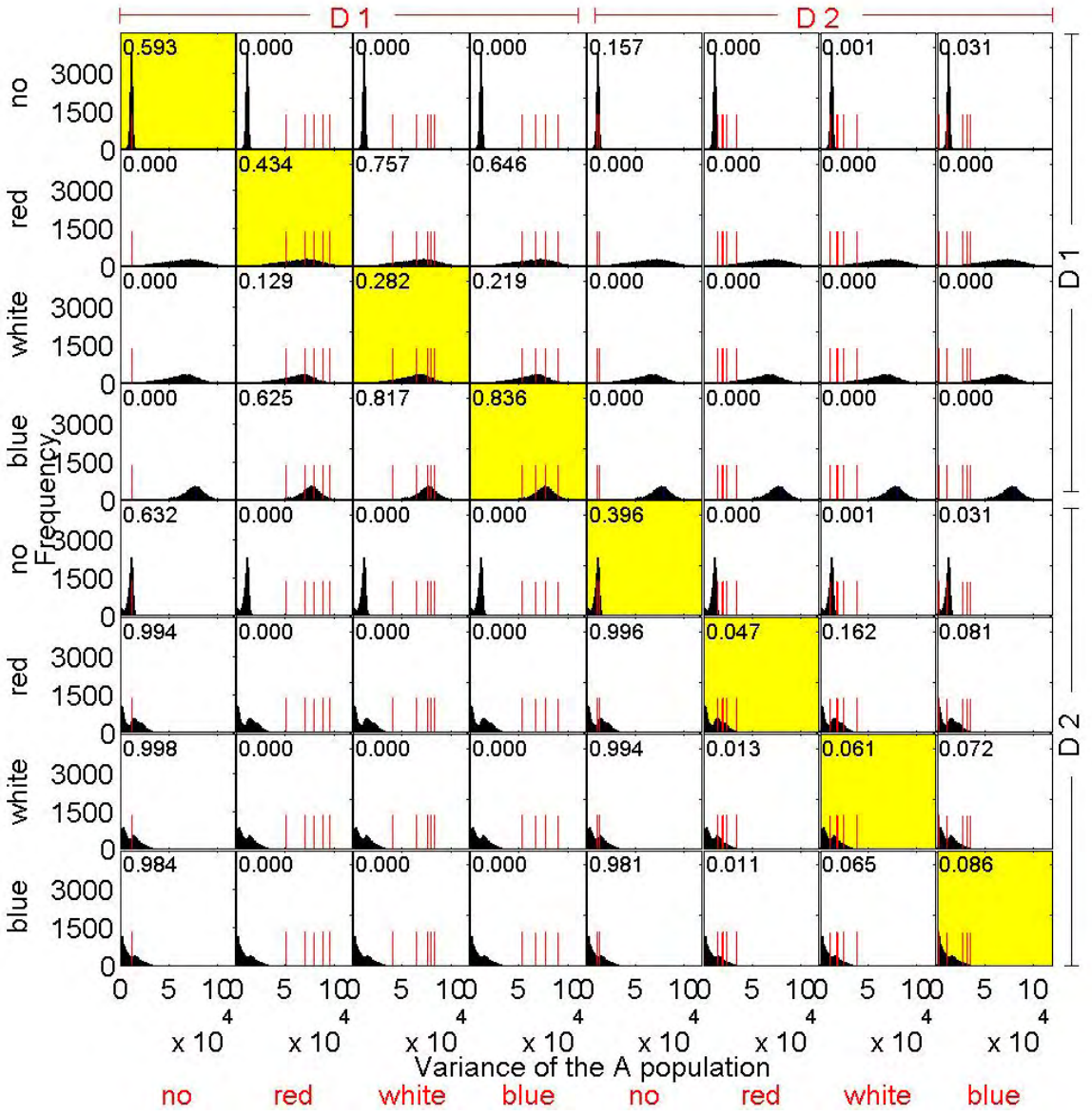
D 1
D 2
0.593
0.000
0.000
0.000
0.157
0.000
0.001
0.031
0.000
0.434
0.757
0.646
0.000
0.000
0.000
0.000
0.000
0.129
0.282
0.219
0.000
0.000
0.000
0.000
0.000
0.625
0.817
0.836
0.000
0.000
0.000
0.000
0.632
0.000
0.000
0.000
0.396
0.000
0.001
0.031
0.994
0.000
0.000
0.000
0.996
0.047
0.162
0.081
0.998
0.000
0.000
0.000
0.994
0.013
0.061
0.072
0.984
0.000
0.000
0.000
0.981
0.011
0.065
0.086
no
red
white
blue
Frequency
3000
1500
0
0 5 10
x 10^4
Variance of the A population
no
red
white
blue

240 **I**

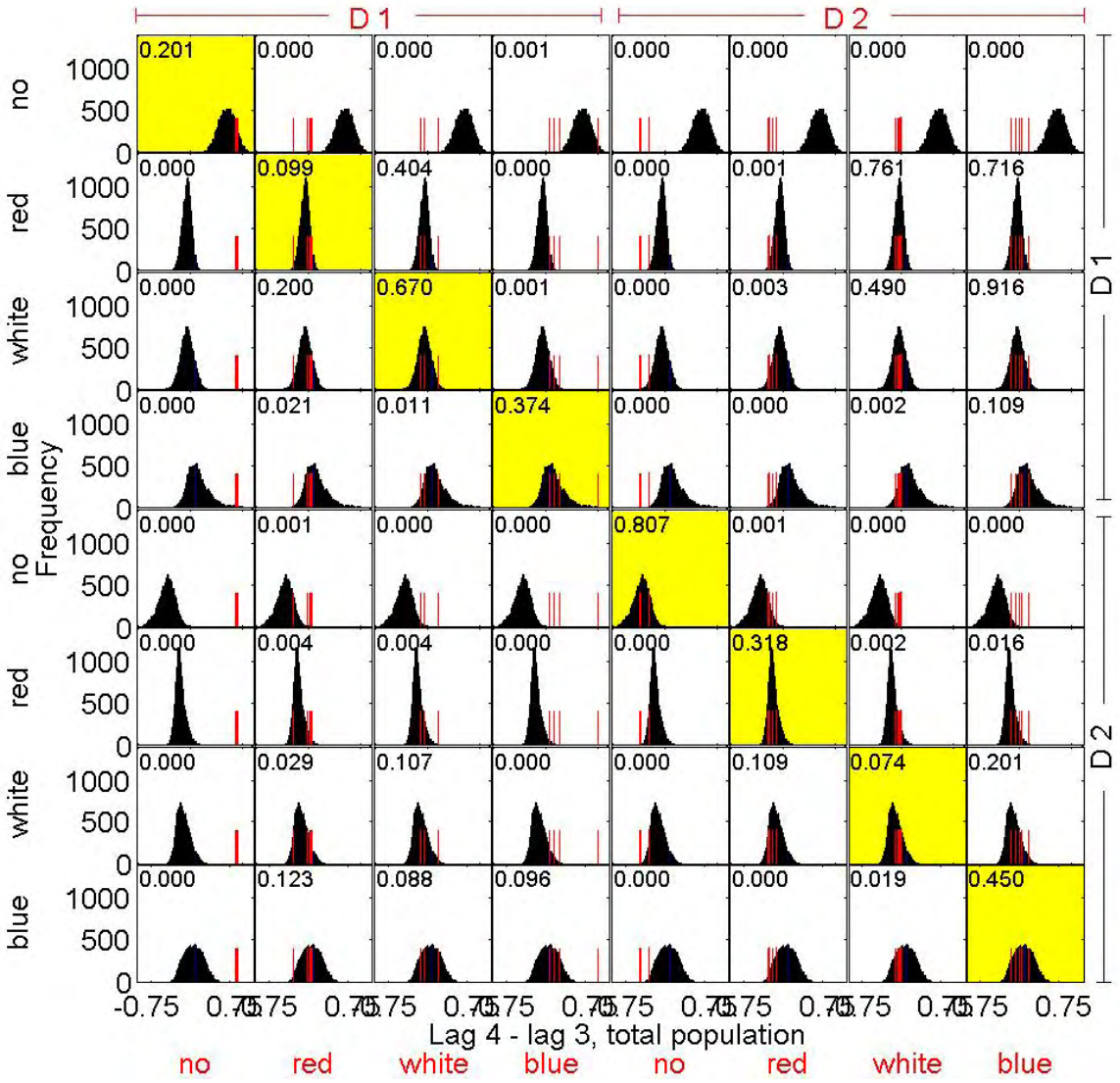
D 1
D 2
no
red
white
blue
Frequency
0.201 0.000 0.000 0.001 0.000 0.000 0.000 0.000
0.000 0.099 0.404 0.000 0.000 0.001 0.761 0.716
0.000 0.200 0.670 0.001 0.000 0.003 0.490 0.916
0.000 0.021 0.011 0.374 0.000 0.000 0.002 0.109
0.000 0.001 0.000 0.000 0.807 0.001 0.000 0.000
0.000 0.004 0.004 0.000 0.000 0.318 0.002 0.016
0.000 0.029 0.107 0.000 0.000 0.109 0.074 0.201
0.000 0.123 0.088 0.096 0.000 0.000 0.019 0.450
1000
500
0
-0.75
0.75
Lag 4 - lag 3, total population

241

242 **J**

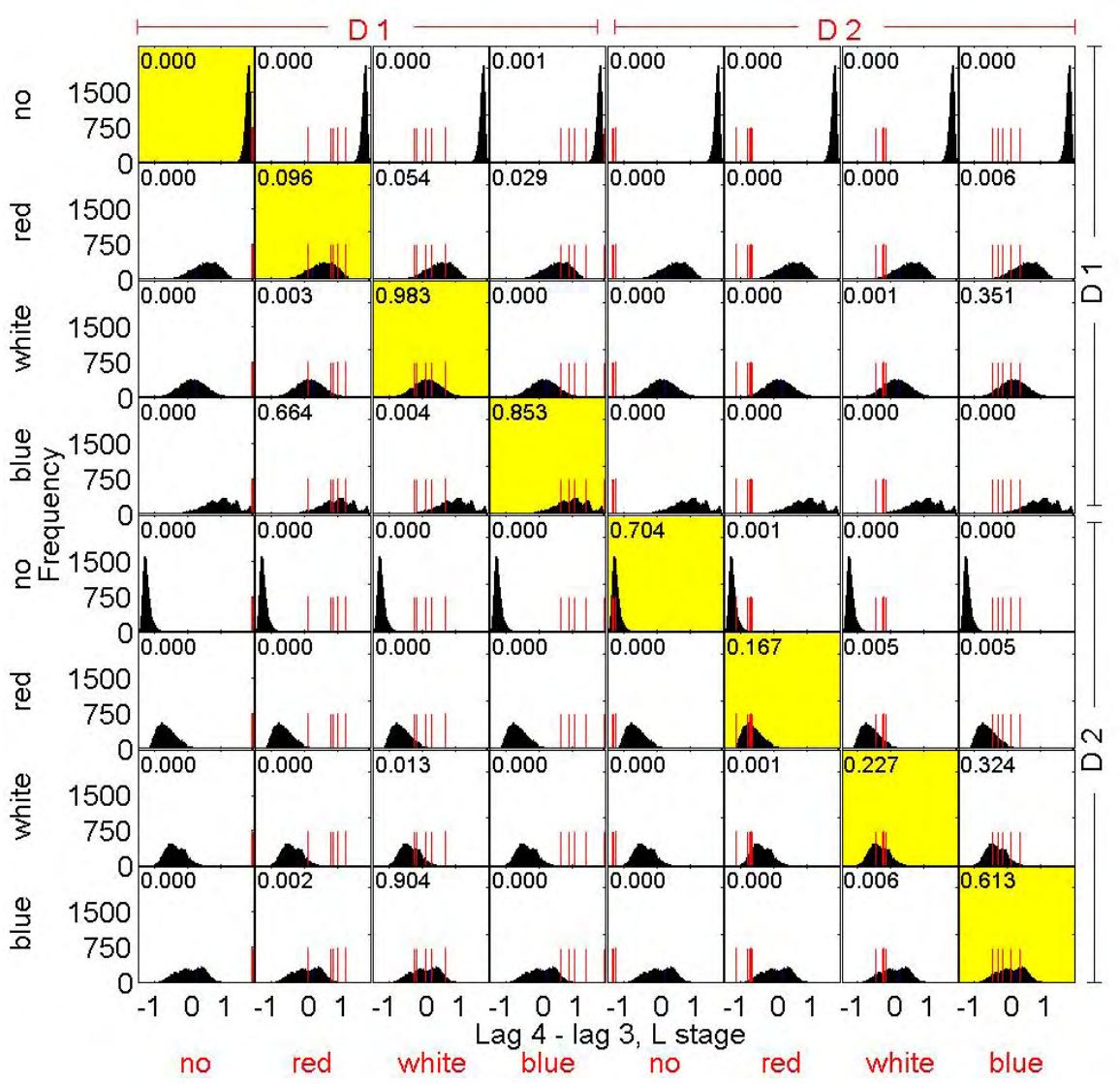
D 1
D 2
no
red
white
blue
Frequency
1500
750
0
0.000 0.000 0.000 0.001 0.000 0.000 0.000 0.000
0.000 0.096 0.054 0.029 0.000 0.000 0.000 0.006
0.000 0.003 0.983 0.000 0.000 0.000 0.001 0.351
0.000 0.664 0.004 0.853 0.000 0.000 0.000 0.000
0.000 0.000 0.000 0.000 0.704 0.001 0.000 0.000
0.000 0.000 0.000 0.000 0.000 0.167 0.005 0.005
0.000 0.000 0.013 0.000 0.000 0.001 0.227 0.324
0.000 0.002 0.904 0.000 0.000 0.000 0.006 0.613
-1 0 1
Lag 4 - lag 3, L stage
no red white blue no red white blue

243

244 **K**

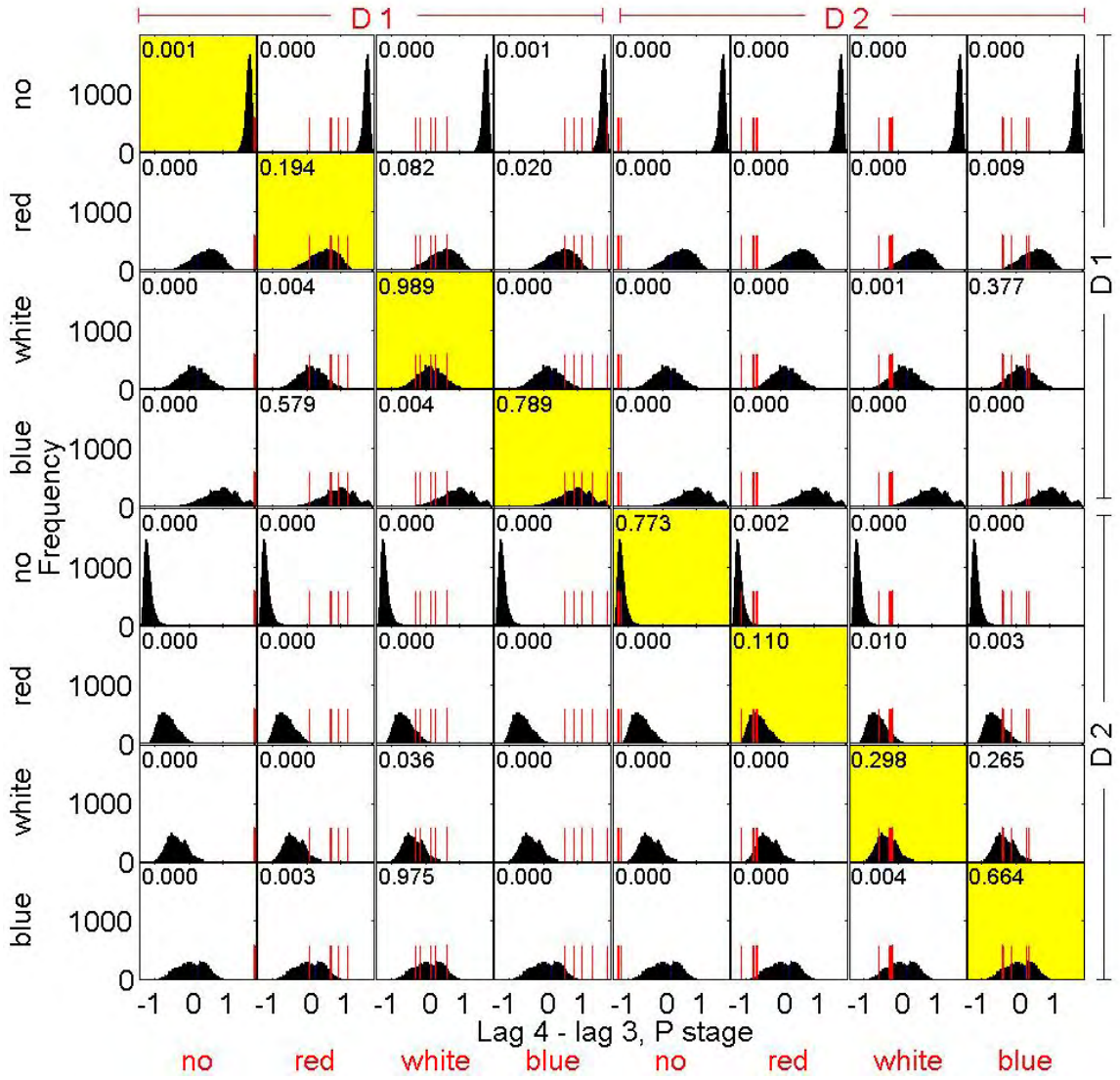
D 1
D 2
no
red
white
blue
Frequency
1000
0
0.001 0.000 0.000 0.001 0.000 0.000 0.000 0.000
0.000 0.194 0.082 0.020 0.000 0.000 0.000 0.009
0.000 0.004 0.989 0.000 0.000 0.000 0.001 0.377
0.000 0.579 0.004 0.789 0.000 0.000 0.000 0.000
0.000 0.000 0.000 0.000 0.773 0.002 0.000 0.000
0.000 0.000 0.000 0.000 0.000 0.110 0.010 0.003
0.000 0.000 0.036 0.000 0.000 0.000 0.298 0.265
0.000 0.003 0.975 0.000 0.000 0.000 0.004 0.664
-1 0 1
Lag 4 - lag 3, P stage
no red white blue no red white blue

245

246 **L**

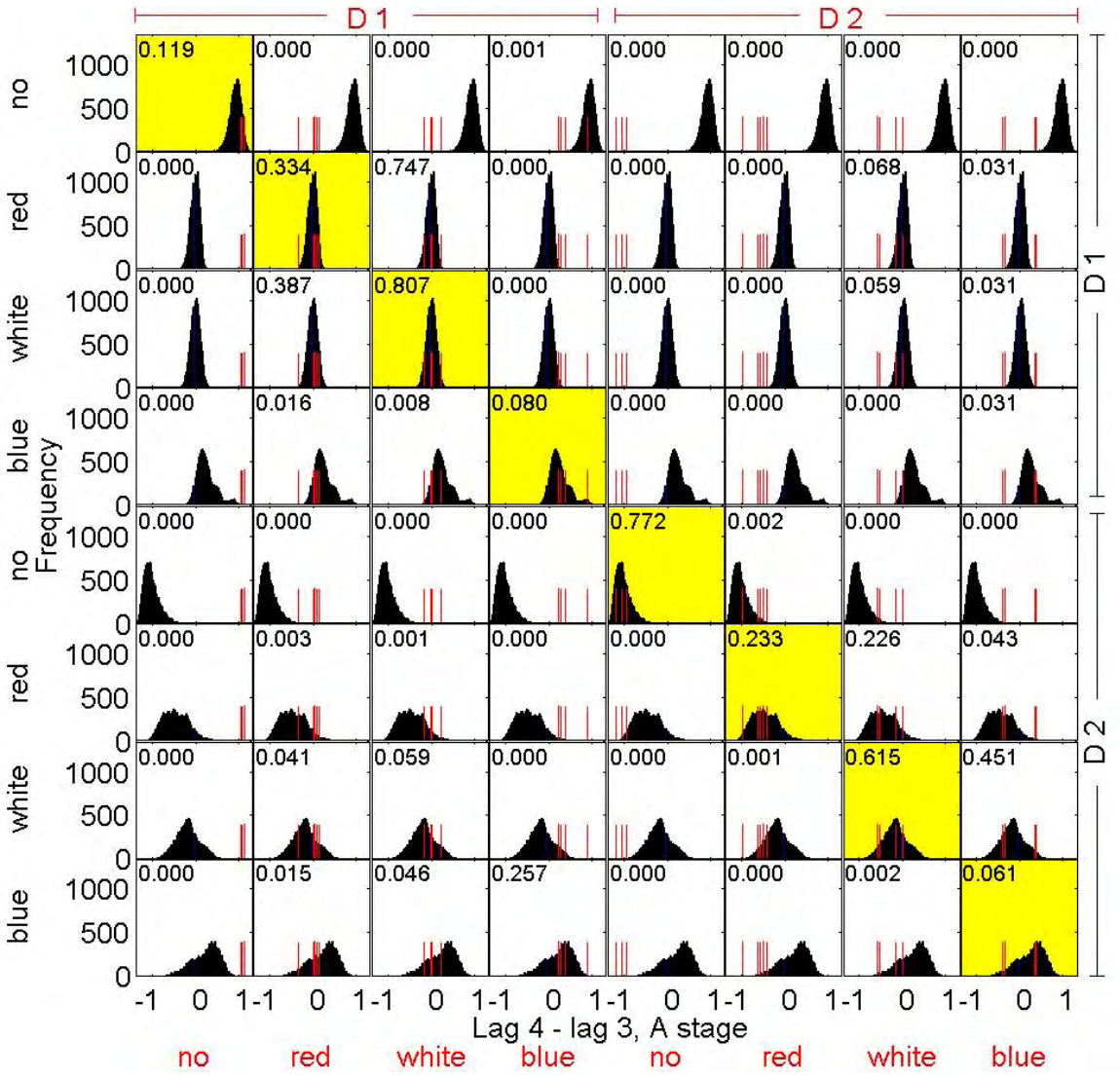
D 1
D 2
no
red
white
blue
Frequency
1000
500
0
0.119 0.000 0.000 0.001 0.000 0.000 0.000 0.000
0.000 0.334 0.747 0.000 0.000 0.000 0.068 0.031
0.000 0.387 0.807 0.000 0.000 0.000 0.059 0.031
0.000 0.016 0.008 0.080 0.000 0.000 0.000 0.031
0.000 0.000 0.000 0.000 0.772 0.002 0.000 0.000
0.000 0.003 0.001 0.000 0.000 0.233 0.226 0.043
0.000 0.041 0.059 0.000 0.000 0.001 0.615 0.451
0.000 0.015 0.046 0.257 0.000 0.000 0.002 0.061
-1 0 1
Lag 4 - lag 3, A stage

247

Figure S5: Same as Fig. 4, but for the P stage (A) and the A stage (B). Black lines on each plot correspond to no imposed environmental noise and the control treatments. Red lines correspond to experimentally imposed noise (*V* oscillating stochastically between 80g and 8g). Green lines correspond to moderate environmental noise (*V*=68g or 20g) and blue lines correspond to weak environmental noise (*V*=56g and 32g).

A

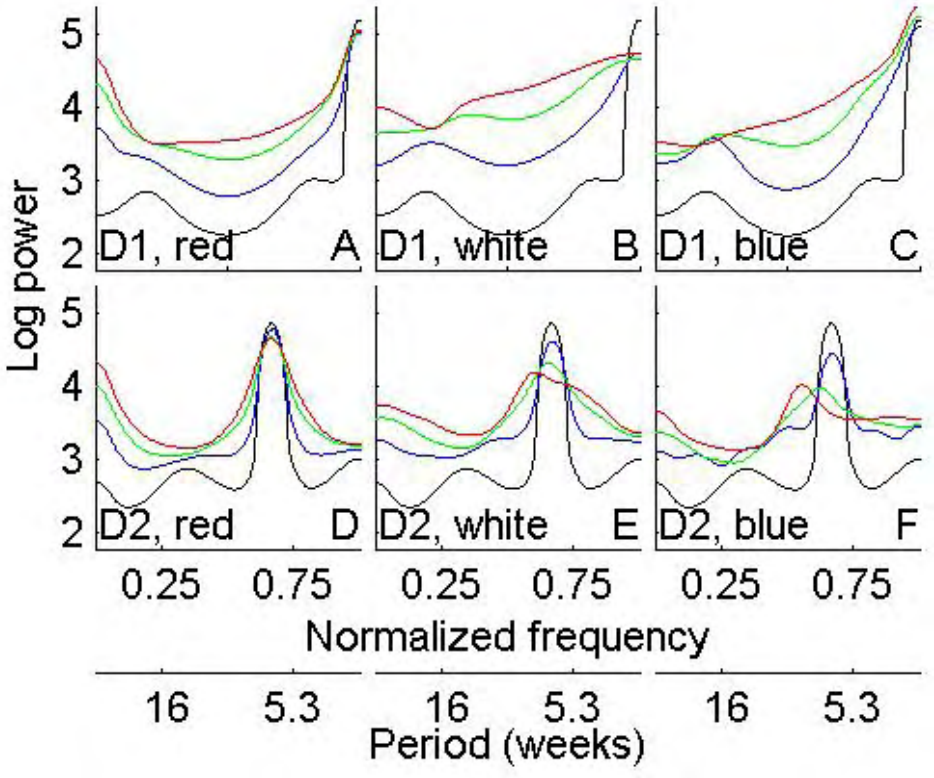

B

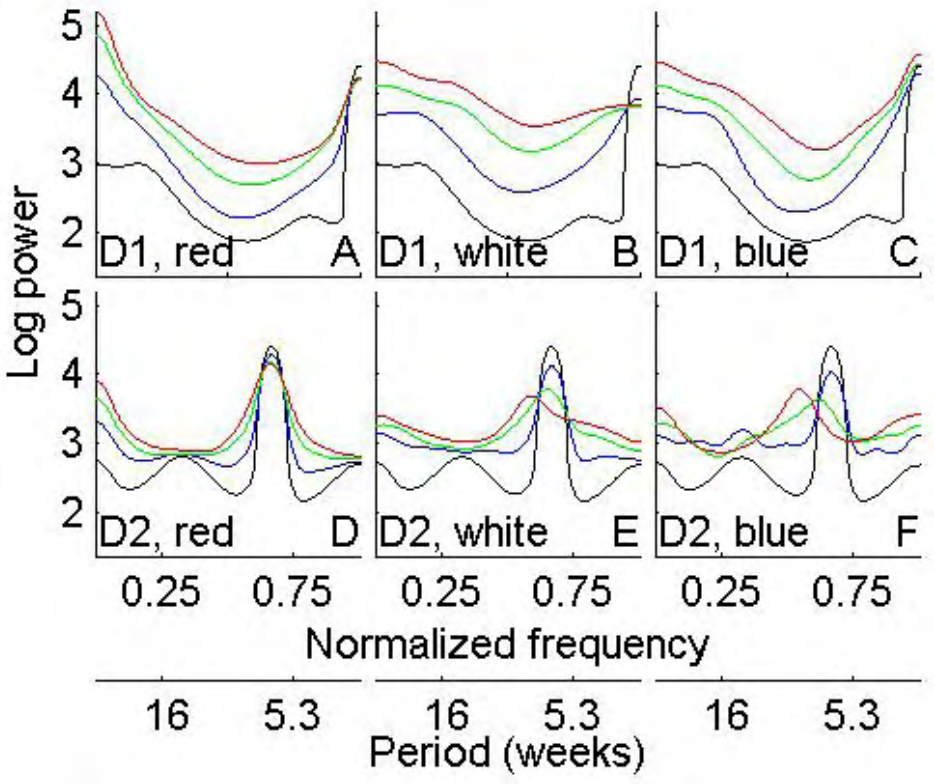
Log power
5
4
3
2
D1, red
A
D1, white
B
D1, blue
C
D2, red
D
D2, white
E
D2, blue
F
0.25
0.75
Normalized frequency
16
5.3
Period (weeks)